THE CALCULATION OF ELECTRIC MICROFIELD DISTRIBUTIONS

BY

CARLOS A. IGLESIAS

A DISSERTATION PRESENTED TO THE GRADUATE COUNCIL
OF THE UNIVERSITY OF FLORIDA IN
PARTIAL FULFILLMENT OF THE REQUIREMENTS
FOR THE DEGREE OF DOCTOR OF PHILOSOPHY

UNIVERSITY OF FLORIDA

1981

This work is dedicated to the author's parents, Carlos A. Iglesias, Sr., and Lilliam V. Iglesias.

ACKNOWLEDGMENTS

I would like to thank Professor C.F. Hooper, Jr. for suggesting this problem and for his guidance and encouragement during the course of this work. A special thanks is due to Dr. J.W. Dufty for many valuable discussions. Thanks are also due to Dr. Robert L. Coldwell and Lawrence A. Woltz for providing guidance in the numerical work as well as for lending me several excellent computer codes.

The diligence and care with which Ms. Viva Benton typed the manuscript is very gratefully acknowledged.

Finally, a special debt of gratitude is owed to my parents for the special understanding they have shown during the long years of this work.

TABLE OF CONTENTS

Page

ACKNOWLEDGEMENTS.....iii

ABSTRACT.....vi

CHAPTER

I CLUSTER EXPANSION FOR THE MICROFIELD DISTRIBUTION IN A PLASMA.....1

1. Formalism.....2
2. Corrections.....19
3. Results.....25
4. Conclusion.....26

II LOW-FREQUENCY MICROFIELD.....33

1. Line Shape Function.....35
2. Method I: Classical Plasmas.....47
3. Evaluation of $Q_I(\vec{\varepsilon})$ 50
4. Method II.....60
5. Evaluation of $\langle \delta(\varepsilon - \vec{E}_i^{\Sigma}) \rangle_p$ 62
6. The Classical Limit.....69
7. Comparisons of the Methods.....71
8. Summary.....75

III QUANTUM CORRECTIONS TO THE LOW-FREQUENCY COMPONENT MICROFIELD DISTRIBUTION.....76

1. Low-Frequency Microfield Distribution.....77
2. Effective Quantum Interaction.....78
3. Numerical Results and Analysis.....82

IV INTEGRAL EQUATION METHOD.....89

1. Connection with the Chemical Potential.....89
2. The Two-Body Function $g(\vec{r};\zeta)$ 91
3. The Holtsmark Limit.....93
4. HNC Approximation.....94
5. Alternate Approximation Schemes.....100

APPENDICES

A DERIVATION OF EFFECTIVE INTERACTIONS.....103

B EVALUATION OF $T_o(\ell)/T_o(0)$ 105

C CALCULATION OF γ_1 107

D CALCULATION OF THE FUNCTIONS t(x) AND p(x).....108

E PROJECTION OPERATOR TECHNIQUES.....110

REFERENCES.....114

BIOGRAPHICAL SKETCH.....118

Abstract of Thesis Presented to the Graduate Council
of the University of Florida in Partial Fulfillment of the
Requirements for the Degree of Doctor of Philosophy

THE CALCULATION OF ELECTRIC
MICROFIELD DISTRIBUTIONS

by

Carlos A. Iglesias

August, 1981

Chairman: Charles F. Hooper, Jr.
Major Department: Physics

This work is a study of electric microfield distribution functions in a plasma. The first work on this problem was done by Holtsmark, who assumed all particles to be statistically independent. Since then, various attempts have been made to include correlations between the particles. This work employs a virial-Debye chain cluster expansion to reinterpret a collective coordinate approach to the microfield distributions developed by Hooper.

The electric microfield distributions have been used in the calculations of the broadening of spectral lines emitted by atoms or ions in a plasma. The application of these distributions to the line shape problem is usually accompanied with two assumptions: (1) neglect of ion motion, and (2) neglect of the ion-electron interactions and their effect approximated by a shielding of the ion-ion interactions. Here, the microfield distribution formalism for the line shape function is retained but without assumptions (1) and (2). With this approach it

is now possible to investigate an aspect of the line broadening problem which in the past has been frequently neglected in the usual line-shape theories. The point in question is the ad hoc introduction of the screened ion fields by the usual line-shape theories which treats incorrectly the electron width and shift operator. The systematic introduction of the shielded ion microfield clearly shows that the form of the electron width and shift operator is more complicated than in the usual theories.

Because of assumption (2), the ion electric microfield distribution used in the line shapes have a shielded ion field. The electron shielding of the ions is usually taken to be the Debye-Hückel result which applies for a classical picture of the electrons. A study of quantum corrections to the electron screening of the ions in the microfield distributions including numerical results is presented.

An integral equation method for evaluating the microfield distributions is proposed. The method is shown to simplify in the hypernetted-chain approximation.

CHAPTER I
CLUSTER EXPANSION FOR THE MICROFIELD DISTRIBUTION IN A PLASMA

The electric microfield distribution function was first calculated by Holtsmark,[1] who solved it by neglecting the correlations between the various charged particles producing the electric field. Since then, various attempts have been made to include these correlations.[2-8] The purpose of this chapter is to reinterpret a collective coordinate approach to the microfield distribution developed by Hooper.[5] We will show that the method employed in Ref.5, hereafter referred to as I, is equivalent to a combined virial-Debye expansion similar to that developed by Mayer.[9]

The system that we deal with consists of N charge particles immersed in a uniform neutralizing background. In addition, when treating the problem of the electric field distribution at a charged point, a "zeroth" particle must be included. The N+1 particles interact through the Coulomb potential. The total system is assumed to be in thermal equilibrium and macroscopically neutral.

The reinterpretation will start by expressing the high-frequency[3] component electric microfield distribution in a cluster expansion similar to the classical expansions of Ursell and Mayer.[10] Then, a split of the central interactions into a long-ranged and a short-ranged contribution is introduced as in I. A central interaction involves the zeroth particle and one of the N charged particles; a noncentral interaction involves any pair from the N charged particles. The

long-ranged central and noncentral interactions we treat in a Debye-chain expansion,[11] since these interactions of infinite range display collective effects. The short-ranged central and the screened interactions from the Debye-chain sums we treat in a virial expansion.[9] We stress that although similar in technique, the cluster expansion presented here is different from previous developements.[2,3,5] Corrections to I which result from retaining additional correlations are presented.

I.1 Formalism

Define $Q(\vec{\varepsilon})$ as the probability of finding an electric field $\vec{\varepsilon}$, at a singly charged point located at $\vec{r}_o$ due to N charged particles moving in a uniform neutralizing background and contained in a volume Ω. Then, if Z represents the configurational partition function of the N+1 particle system, we may write

$$Q(\vec{\varepsilon}) = Z^{-1} \int\cdots\int d\vec{r}_o \, d\vec{r}_1 \cdots d\vec{r}_N \, e^{-\beta V} \, \delta(\vec{\varepsilon} - \vec{E}) \tag{1.1.1}$$

where $\vec{r}_j$ represents the coordinate of the j^{th} particle, $\beta=(kT)^{-1}$, V the potential energy of the system, and $\vec{E}$ is the electric field at $\vec{r}_o$ due to the N charged particles in a given coordinate configuration.

The potential energy of the system, V, is expressed as

$$V = \sum_{0=i<j}^{N} e^2/r_{ij} + V_B, \tag{1.1.2}$$

where V_B represents the contributions to the potential energy due to the neutralizing background.

An expression for V in terms of a Fourier expansion results in

$$V = \frac{4\pi e^2}{\Omega} \sum_{k\neq 0} \sum_{0=i<j}^{N} e^{-i\vec{k}\cdot\vec{r}_{ij}}/k^2 , \tag{1.1.3}$$

where the exclusion of the $\vec{k}=0$ term in Eq.(1.1.3) accounts for the neutralizing background.[2]

Assuming that our system is isotropic we may rewrite[2] Eq.(1.1.1) as

$$P(\varepsilon) = 2\pi^{-1}\varepsilon \int_0^\infty d\ell\,\ell T(\ell)\sin(\varepsilon\ell) \tag{1.1.4}$$

where $P(\varepsilon)$ is related to $Q(\vec{\varepsilon})$ by the relation,

$$4\pi Q(\vec{\varepsilon})\varepsilon^2 d\varepsilon = P(\varepsilon)d\varepsilon; \tag{1.1.5}$$

$T(\ell)$ is defined by,

$$T(\ell) \equiv Z(\ell)/Z, \tag{1.1.6}$$

$$Z(\ell) \equiv \int\cdots\int d\vec{r}_o\, d\vec{r}_1\cdots d\vec{r}_N\, e^{-\beta V(\ell)}, \tag{1.1.7}$$

$$V(\ell) \equiv \sum_{0=i<j}^{N} v_{ij}(\ell) = \sum_{0=i<j}^{N} \left(1 - \frac{i\,\vec{\ell}\cdot\vec{\nabla}_o}{e\beta}\right)v_{ij}, \tag{1.1.8}$$

where $v_{ij} = e^2/r_{ij}$ and $\vec{\nabla}_o$ is the gradient with respect to the zeroth particle.

The function $Z(\ell)$ has the form of a configurational partition function with the "potential energy" of the system $V(\ell)$, defined in Eq.(1.1.8). We proceed to calculate numerator and denominator of

Eq.(1.1.6) using the classical cluster expansions for configurational partition functions which were developed by Ursell and Mayer.[10]

Again noting that the numerator $Z(\ell)$ has the form of a configurational partition function, we write it in the form of a "Helmholtz free energy," $F(\ell)$:

$$Z(\ell) = e^{-\beta F(\ell)}; \tag{1.1.9}$$

$F(\ell)$ given by,

$$-\beta F(\ell) = \Omega\, A(\rho,\ell). \tag{1.1.10}$$

Now the quantity A can be expressed in terms of a cluster expansion,[10]

$$A(\rho,\ell) = \sum_{n=2}^{N} \frac{\rho^n}{n!} \int\cdots\int R(\mathbf{n},\ell) \prod_{j}^{n} d\vec{r}_j. \tag{1.1.11}$$

Here, $R(\mathbf{n},\ell)$ is the sum of all products of f-Mayer functions in which every particle in $\mathbf{n}$ is independently connected to every other particle in $\mathbf{n}$. The f-Mayer functions are defined as

$$f_{ij}(\ell) = (e^{-\beta v_{ij}(\ell)} - 1) \tag{1.1.12}$$

where

$\mathbf{n}$ = set of $n = n_o + n_i$ particles

$\mathbf{n!} = n_o! n_i!$

$\rho^n = \rho_o^{n_o} \rho^{n_i}$; $\rho_o = \Omega^{-1}$, $\rho = N/\Omega$

$$\int\cdots\int \prod_{j}^{n} d\vec{r}_j = \text{integrations over set of n particles} \qquad (1.1.13)$$

n_o and n_i are the number of zeroth particles, here equal to 0 or 1, and N charged particles in the cluster $R(\mathbf{n},\ell)$, respectively.

The clusters in the expansion of $A(\rho,\ell)$ are of two types:

(1) Clusters which do not contain the zeroth particle, $n_o=0$.

(2) Clusters which do contain the zeroth particle, $n_o=1$.

If $A_1(\rho)$ and $A_2(\rho,\ell)$ denote the contributions from all type (1) and (2) clusters, respectively, then

$$Z(\ell) = \exp\{\Omega A_1(\rho) + \Omega A_2(\rho,\ell)\}. \qquad (1.1.14)$$

A similar procedure can be applied to $Z = Z(\ell=0)$, with the result

$$Z(\ell=0) = \exp\{\Omega A_1(\rho) + \Omega A_2(\rho,0)\}. \qquad (1.1.15)$$

The term $A_1(\rho)$ is independent of ℓ; in fact, $\exp(\Omega A_1(\rho))$ is the configurational partition function for the plasma without the zeroth particle.

Substituting Eq.(1.1.14) and Eq.(1.1.15) in Eq.(1.1.6) allows us to write

$$T(\ell) = \exp\{\Omega(A_2(\rho,\ell) - A_2(\rho,0)\}\ . \qquad (1.1.16)$$

That is, all clusters not involving the zeroth particle cancel exactly in Eq.(1.1.16).

A graphical representation[10] of some of the terms appearing in A_2 is shown in Fig. (1.1); a black vertex represents one of the N charged particles, a white vertex the zeroth particle. Each f-Mayer function is represented by a heavy-solid line connecting two vertices.

As in I, we conjecture that quantitative features of the microfield distribution will be more sensitive to central than to noncentral interactions. A central interaction involves the zeroth particle and one of the N charged particles; a noncentral interaction involves any pair of N charged particles. Based on this conjecture, the details of the central interactions are treated with greater care. Therefore, we split the central interactions into long- and short-range contributions. The long-range central and all of the noncentral coulomb interactions we treat in a Debye-chain[11] expansion. After the long-range contributions are renormalized, all the remaining short-range "interactions" are treated by means of a virial expansion. From an examination of the formalism it is clear that the two expansions are not independent, but involve a hybrid (virial/Debye) cluster expansion. It must be emphasized that the conjecture discussed above is based on a plausibility argument, which is justified by results.[5-7] To carry out this procedure, we first set

$$v_{oj} = u_{oj} + w_{oj} \tag{1.1.17}$$

where

$$w_{oj} = (e^2/r)e^{-\alpha r_{oj}/\lambda} . \tag{1.1.18}$$

In Eq.(1.1.18) α is an arbitrary, real, positive parameter which will be independently determined, and λ is the Debye length,

Fig. 1.1 Graphical representation of A_2. A black vertex represents an ion, a white vertex the zeroth particle. Each f-Mayer function is represented by a heavy-solid line connecting two vertices.

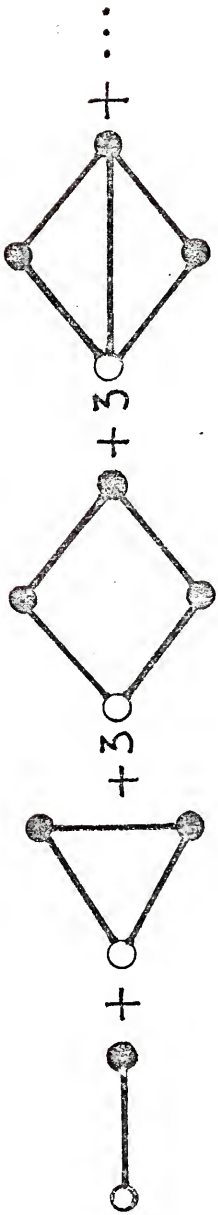
+
+3
+3
+ ...

$$\lambda = (4\pi e^2 \rho\beta)^{-1/2} . \tag{1.1.19}$$

Substitute Eq.(1.1.17) into the expression for the f-Mayer functions, Eq.(1.1.12). This yields a result similar to one used by Mayer[9] but with the difference that in the present paper only central interactions are split

$$f_{ij}(\ell) = \begin{cases} (e^{-\beta v_{ij}} - 1) & i,j \neq 0 \\ \chi_j(\ell) + [1 + \chi_j(\ell)] \sum_{n=1}^{\infty} [-\beta u_{oj}(\ell)]^n/n! & \begin{matrix} i=0 \\ j\neq 0 \end{matrix} \end{cases} \tag{1.1.20}$$

where

$$\chi_{ij}(\ell) = (e^{-\beta w_{oj}(\ell)} - 1). \tag{1.1.21}$$

With the aid of Eq.(1.1.20) we may further separate the products in $R(\rho,\ell)$ into sums of products involving the f-function, χ-function, and $[-\beta u]^n/n!$ functions represented by heavy-solid lines, light-solid lines, and n-dashed lines, respectively. Clearly, there can be at most one f or χ bond directly connecting two vertices. The result of splitting the central interactions is shown graphically for some 2 and 3 particle clusters in Fig.(1.2a). The two $(-\beta u)$-bonds with the triple dot in between represent the sum of graphs with all possible number of $(-\beta u)$-bonds as shown in Fig. (1.2b).

In order to perform a Debye-chain expansion on the long-range central and noncentral interactions we expand the noncentral f-Mayer functions in powers of $(-\beta v)$. With the decomposition of the f-functions into powers of $(-\beta v)$ functions we can sum simple chains of

$(-\beta u)$- and $(-\beta v)$-bonds as shown in Fig. (1.3). Two types of chains are possible: the first has the zeroth particle and one perturbing ion for endpoints, while the second has two ions for endpoints. It is understood that the two vertices at the endpoints of Fig. (1.3) are in general part of a more complicated graph. Hence, we are summing all graphs which are the same except for the one sum of interactions displayed. The intermediate ions in Fig. (1.3) do not interact with any particles except as explicitly shown in the figure. The final form for A_2 is an infinite series of integrals involving products of the functions, χ, u^s, and v^s; u^s and v^s are defined graphically in Fig. (1.3) and evaluated in Appendix A. There is the restriction that no simple chains in the effective interactions u^s and v^s appear in A_2 because such a chain is in effect a simple chain in u and v interactions which have been already included in the summations. The new cluster expansion for A_2 is given by

$$\Omega A_2(\rho,\ell) = \ell n\, T_o(\ell) + \sum_{n=1}^{\infty} \frac{\rho^n}{n!} h_n(\ell), \qquad (1.1.22)$$

where $\ell n\, T_o(\ell)$ is the contribution from the ring graphs presented graphically in Fig.(1.4a), and h_n is the set of all n+1 particle clusters, excluding ring graphs, involving products of the functions χ, u^s, and v^s as described above and presented graphically in Fig.(1.4b) and (1.4c) for n=1 and 2.

In Fig.(1.4) we have separated the graphs for n=1 and 2 into the subsets (b1,b2) and (c1,c2). The separation is employed since it can be shown that only the graphs shown in (b1), (c1) are included in I. There, only the first term in the Gram Charlier[12] expansion series for

Fig. 1.2 Some 2 and 3 particle clusters in A_2 after the splitting of central interactions. The f-Mayer, χ, and $(-\beta u)^n/!$ functions are represented by heavy-solid lines, and n dashed lines, respectively.

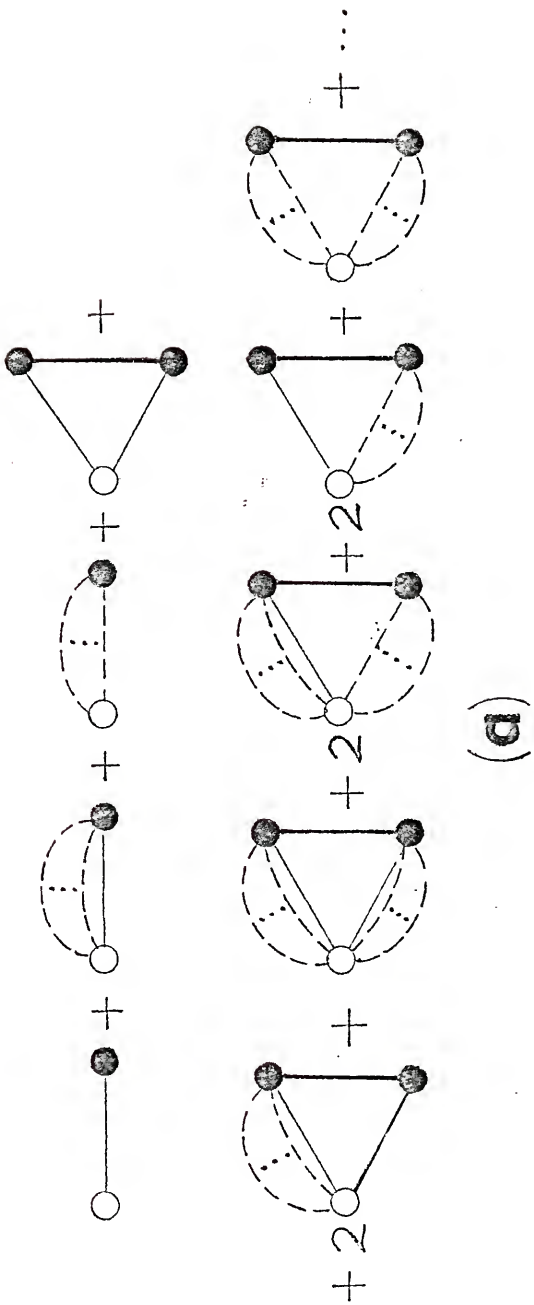
2
2
2
(a)
(b)

Fig. 1.3 The effective interactions u^S and v^S.

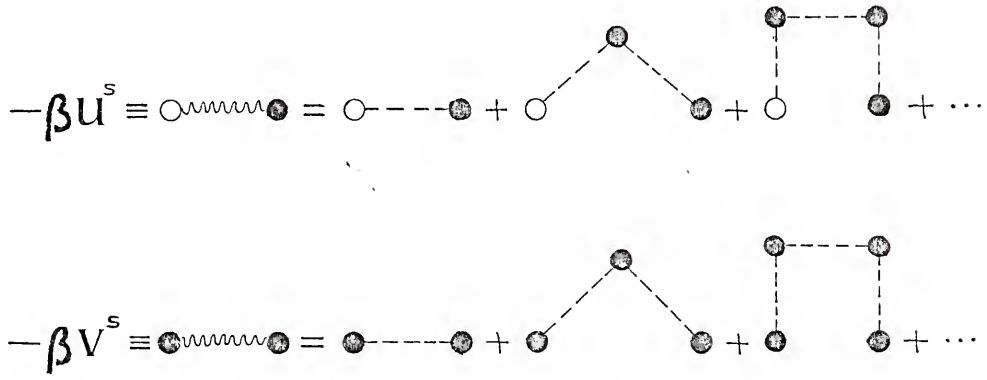

Fig. 1.4 The contributions to A_2 up to n=2 of Eq. (1.1.22). (a) The ring graphs. (b1) and (c1) re the graphs included in the Jacobian approximation in I. (b2) and (c2) are the neglected terms in I. The triple dot has the same meaning here as in Fig. (2), except now it involves $(-\beta u^2)$-bonds. Note that the noncentral bonds in the second bracket of (c2) have a minimum of two $(-\beta u^s)$-bonds. The graph in (b2) has a minimum of three $(-\beta u^s)$-bonds.

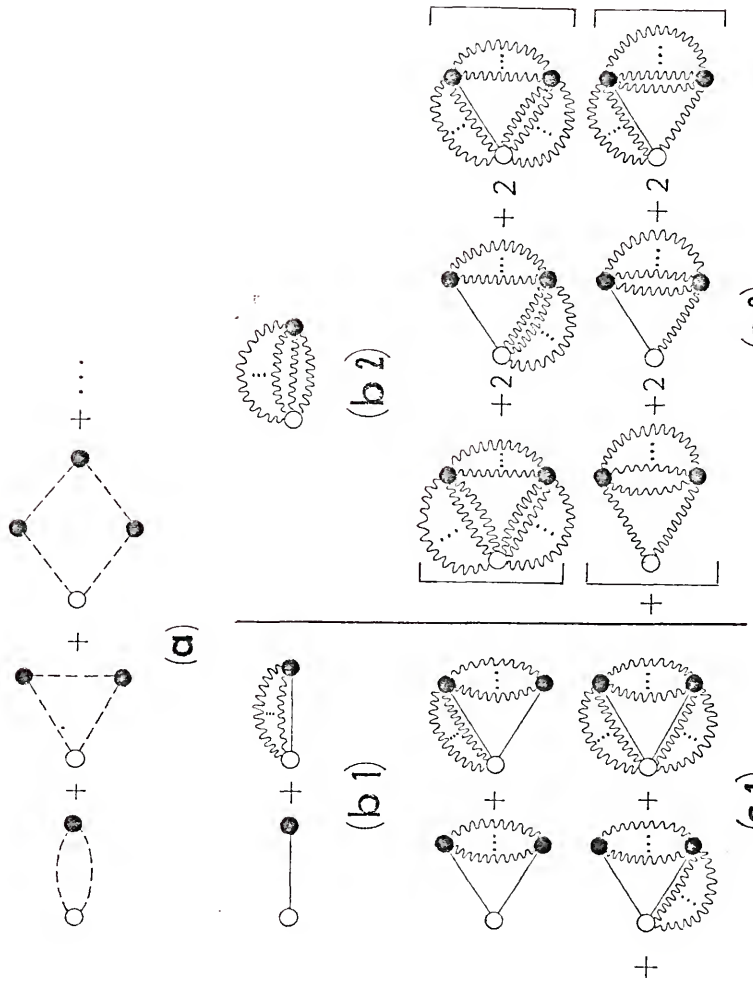
(a)
(b 1)
(b 2)
(c 1)
(c 2)
2
2
2

the Jacobian of the collective coordinate transformation is retained. We will show that the graphs (b2) and (c2) are neglected by such an approximation.

Splitting up the potential appearing in $Z(\ell=0)$ in the same manner as previously described in treating $Z(\ell)$, we are able to carry out a similar expansion program with the result

$$\Omega A_2(\rho,0) = \ell n\, T_o(0) + \sum_{n=1}^{\infty} \frac{\rho^n}{n!} h_n(0). \qquad (1.1.23)$$

The graphs representing the terms in Eq.(1.1.23) are topologically equivalent to those in Eq.(1.1.22) but with ℓ set equal to zero.

Combining Eqs.(1.1.16), (1.1.22). and (1.1.23) gives the following result for $T(\ell)$:

$$T(\ell) = [T_o(\ell)/T_o(0)] \exp\left\{ \sum_{n=1}^{\infty} \frac{\rho^n}{n!} [h_n(\ell) - h_n(0)]\right\}. \qquad (1.1.24)$$

Now consider the individual terms appearing in Eq.(1.1.24). In Appendix B we show that the first term, $T_o(\ell)/T_o(o)$, can be written as

$$T_o(\ell)/T_o(0) = \exp\{-\gamma L^2\}. \qquad (1.1.25)$$

In Eq.(1.1.25),

$$L = \ell\varepsilon_o,\ \gamma = a\alpha^3/4(\alpha^2+1)^2,\ a = r_o/\lambda,\ \text{and}\ \varepsilon_o = e/r_o^2; \qquad (1.1.26)$$

r_o is the ion sphere radius defined by the expression

$$\frac{4\pi}{3} r_o^3 \rho = 1. \tag{1.1.27}$$

Next, we consider the factors resulting from terms in the series exponent. For n=1, and considering only terms shown graphically in Fig.(1.4b1), we write

$$I_1^{(1)}(\ell) = \rho\{h_1^{(1)}(\ell) - h_1^{(1)}(0)\}$$

$$= \rho \int d\vec{r}_{10} \{\chi_1(\ell)Q_1(\ell) - \chi_1(0)Q_1(0)\}$$

$$= 3 \int_o^\infty dx\, x^2\{e^{F(x)}\left(\frac{\sin[LG(x)]}{LG(x)} - 1\right) - e^{s(x)}\left(\frac{\sin[Lq(x)]}{Lq(x)} - 1\right)\} \tag{1.1.28}$$

where the angular integrations have been done. The functions in the second equality are defined by

$$Q_1(\ell) = \exp\{-\beta u^s(\vec{r}_{10},\ell)\} \tag{1.1.29}$$

$$u^s(\vec{r}_{10},\ell) = [1 - \frac{i\vec{\ell}}{e\beta} \cdot \vec{\nabla}_o]\, u^s(r_{10}). \tag{1.1.30}$$

The functions in the third equality are defined in the next section, Eqs.(1.2.4), (1.2.5), (1.2.7) and (1.2.8).

For the second term in the series, n=2, we use the graphs in Fig. (1.4c1) to write

$$I_2^{(1)}(\ell) = \frac{\rho^2}{2} [h_2^{(1)}(\ell) - h_2^{(1)}(0)]$$

$$= \frac{\rho^2}{2} \iint d\vec{r}_{10} d\vec{r}_{20} [\chi_1(\ell)\chi_2(\ell)Q_1(\ell)Q_2(\ell) -$$

$$- \chi_1(0)\chi_2(0)Q_1(0)Q_2(0)](e^{-\beta v^s_{12}} - 1). \qquad (1.1.31)$$

Thus, the contributions to $T(\ell)$ from Figs.(1.4a), (1.4b1), and (1.4c1) are given by

$$T^{(1)}(\ell) = \exp[-\gamma L^2 + I_1^{(1)}(\ell) + I_2^{(1)}(\ell)]. \qquad (1.1.32)$$

The results in Eqs.(1.1.25-1.1.32) are identical to those in I for $T(\ell)$ as given in Eqs.(25-35) of I.

I.2 Corrections

In Section I.1 we expressed the microfield distribution function in terms of a cluster expansion where the long-range interactions are treated in a Debye-chain expansion and the short-range interactions in a virial expansion. The two are not independent but involve a hybrid virial Debye-chain cluster expansion with the long-range collective effects of the Debye-chains modifying the short-range virial expansion.

As mentioned earlier, the graphs in Figs.(1.4b2 and 1.4c2) are not included in the results of Eq.(1.1.32). The neglected terms can be interpreted as correlations between the collective coordinates introduced in I. In this section we will evaluate these contributions to $T(\ell)$ for n=1 and 2 in Eq.(1.1.24).

The corrections to $I_1(\ell)$, shown graphically in Fig.(1.4b2), is given by

$$I_1^{(2)}(\ell) = \rho[h_1^{(2)}(\ell) - h_1^{(2)}(0)]$$

$$= \rho \int d\vec{r}_1 \{[e^{-\beta u^s(\vec{r}_1,\ell)} - \tfrac{1}{2}(\beta u^s(\vec{r}_1,\ell))^2$$

$$+ \beta u^s(\vec{r}_1,\ell) - 1] - [e^{-\beta u^s(r_1)} - \tfrac{1}{2}(\beta u^s(r_1))^2 + \beta u^s(r_1) - 1]\}. \tag{1.2.1}$$

Performing the angular integrations we get,

$$I_1^{(2)}(\ell) = 3\int_o^\infty dx\, x^2\{e^{s(x)}\left(\frac{\sin[Lq(x)]}{Lq(x)} - 1\right) + \frac{L^2q^2(x)}{6}\} \tag{1.2.2}$$

The functions that appear in the integrand are defined as follows:

$$x = r/r_o \tag{1.2.3}$$

$$s(x) = \frac{\alpha^2}{1-\alpha^2}\left(\frac{a^2}{3x}\right)\left(e^{-ax} - e^{-\alpha ax}\right) \tag{1.2.4}$$

$$q(x) = \frac{\alpha^2}{1-\alpha^2}\left\{\frac{1}{x^2}\left(e^{-\alpha ax} - e^{-ax}\right) - \frac{a}{x}\left(e^{-ax} - e^{-\alpha ax}\right)\right\}. \tag{1.2.5}$$

Combining Eqs.(1.1.28) and (1.2.2) we find that

$$I_1(\ell) = 3\int_o^\infty dx x^2\{e^{F(x)}\left(\frac{\sin[LG(x)]}{LG(x)} - 1\right) + \frac{L^2q^2(x)}{6}\} \tag{1.2.6}$$

with

$$F(x) = \frac{1}{1-\alpha^2}\left(\frac{a^2}{3x}\right)\left(\alpha^2 e^{-ax} - e^{-\alpha ax}\right) \tag{1.2.7}$$

$$G(x) = \frac{1}{1-\alpha^2}\left\{\frac{1}{x^2}\left(e^{-\alpha ax} - e^{-ax}\right) + \frac{a}{x}\left(\alpha e^{-\alpha ax} - \alpha^2 e^{-ax}\right)\right\}. \tag{1.2.8}$$

Before evaluating the contributions from the graphs in Fig.(1.4c) we note that the sum of three particle clusters is a small correction[5] to $T(\ell)$. Hence, we only consider graphs with the lowest nonvanishing number of $(-\beta v^s)$-bonds connecting particles 1 and 2. With this simplification the graphs in Fig.(1.4c) will be of two types: graphs with one $(-\beta v^s)$-bond, and graphs with two $(-\beta v^s)$-bonds.

The contribution to $T(\ell)$ from graphs with one $(-\beta v^s)$-bond is given by

$$I_2^{(1)}(\ell) = \frac{-\beta\rho^2}{2}\int d\vec{r}_1 d\vec{r}_2 v^s(r_{12})\{\chi_1(\ell)\chi_2(\ell)e^{-\beta u^s(\vec{r}_1,\ell)} e^{-\beta u^s(\vec{r}_2,\ell)} - \chi_1(0)\chi_2(0)\, e^{-\beta u^s(r_1)} e^{-\beta u^s(r_2)}\}, \tag{1.2.9}$$

$$I_2^{(2,1)}(\ell) = \frac{-\beta\rho^2}{2}\int d\vec{r}_1 d\vec{r}_2 v^s(r_{12})$$

$$[\{(e^{-\beta u^s(\vec{r}_1,\ell)+\beta u^s(\vec{r}_1,\ell)}-1)(e^{-\beta u^s(\vec{r}_2,\ell)+\beta u^s(\vec{r}_2,\ell)}-1)$$

$$- (e^{-\beta u^s(r_1)} + \beta u^s(r_1) - 1)(e^{-\beta u^s(r_2)+\beta u^s(r_2)}-1)\}$$

$$+ 2\{(e^{-\beta u^s(\vec{r}_1,\ell)+\beta u^s(\vec{r}_1,\ell)} - 1)e^{-\beta u^s(\vec{r}_2,\ell)}\chi_2(\ell)$$

$$- (e^{-\beta u^s(r_1)} + \beta u^s(r_1) - 1)\, e^{-\beta u^s(r_2)}\chi_2(0)\}] \tag{1.2.10}$$

The quantity $I_2^{(1)}(\ell)$ corresponds to the graphs in Fig.(1.4c1) and $I_2^{(2,1)}(\ell)$ to the graphs in the first bracket of Fig.(1.4c2).

The integrands in Eqs.(1.2.9) and (1.2.10) are a product of functions of $(\vec{r}_1,\ell)$ and $(\vec{r}_2,\ell)$ with the exception of the r_{12} coupling term in $v^s(r_{12})$. In order to uncouple the r_1, r_2 dependence, we expand $v^s(r_{12})$ in spherical harmonics.[13]

$$v^s(r_{12}) = -\sum_{k=0}^{\infty}(2k+1)v_k^s(r_1,r_2)P_k(\cos\theta_{12}) \tag{1.2.11}$$

where

$$v_k^s(r_1,r_2) = \frac{a^2}{3} K_{k+1/2}(ax_1)I_{k+1/2}(ax_2)/(x_1x_2)^{1/2} \tag{1.2.12}$$

and $x_j=r_j/r_o$, $x_1>x_2$, and k=0,1,2,.... This method allows Eqs.(1.2.9) and (1.2.10) to be reduced to a tractable double integral where the angular integrations are readily performed to yield

$$I_2^{(1)}(\ell) + I_2^{(2,1)}(\ell) = 3a^2\sum_{k=0}^{\infty}(-1)^k(2k+1)\int_o^{\infty}dx_2x_2^{3/2}I_{k+1/2}(ax_2)$$

$$\times\int_{x_2}^{\infty}dx_1x_1^{3/2}K_{k+1/2}(ax_1)\{i_k^{(1)}(x_1,x_2) + i_k^{(2,1)}(x_1,x_2)\} \tag{1.2.13}$$

$$i_k^{(1)}(x_1,x_2) = e^{s(x_1)}e^{s(x_2)}\{[e^{-\beta w(x_1)}j_k(LG(x_1))-j_k(Lq(x_1))]$$

$$\times [e^{-\beta s(x_2)}j_k(LG(x_2))$$

$$- j_k(Lq(x_2))] - \delta_{k,o}\chi_1(0)\chi_2(0)\} \tag{1.2.14}$$

$$i_k^{(2,1)}(x_1,x_2) = [e^{s(x_2)}\{2e^{-\beta w(x_2)}j_k(LG(x_2))$$

$$- j_k(Lq(x_2))\} - \delta_{k,o}(1+s(x_2))][e^{s(x_1)}j_k(Lq(x_1))-\delta_{k,o}]$$

$$-\delta_{k,o}\{(e^{s(x_1)}-1)[e^{s(x_2)}(2e^{-\beta w(x_2)}-1)-(1+s(\chi_2))]$$

$$+ s(x_1)e^{s(x_2)}[2e^{-\beta w(x_2)}(j_o(LG(x_2))-1) - (j_o(Lq(x_2)) - 1)]\}$$

$$- \frac{L}{3} \delta_{k,1}\{q(x_1)e^{s(x_2)}[2e^{-\beta w(x_2)} j_1(LG(x_2)) - j_1(Lq(x_2))]$$

$$+ q(x_2)[e^{s(x_1)} j_1(Lq(x_1)) - Lq(x_1)/3]\}. \qquad (1.2.15)$$

The functions I and K refer to modified Bessel functions of the first and third kind, respectively, while j_k specifies a spherical Bessel function of order k.[14]

The second bracket in Fig.(1.4c2) shows the graphs with a minimum of two $(-\beta v^s)$-bonds. Their approximate contribution to $T(\ell)$ is given by

$$I_2^{(2,2)}(\ell) = \frac{\rho^2\beta^2}{2} \int d\vec{r}_1 d\vec{r}_2 \, v^s(r_{12})^2$$

$$\times [\frac{\beta^2}{2}\{u^s(\vec{r}_1,\ell)u^s(\vec{r}_2,\ell) - u^s(r_1)u^s(r_2)\}$$

$$-\beta\{u^s(\vec{r}_1,\ell)e^{-\beta u^s(\vec{r}_2,\ell)}\chi_2(\ell) - u^s(r_1)e^{-\beta u^s(r_2)}\chi_2(0)\}]. \qquad (1.2.16)$$

The first term in brackets in Eq.(1.2.15) may be evaluated by introducing the Fourier transforms as shown in Appendix C. Then,

$$\frac{\rho^2\beta^4}{4} \int d\vec{r}_1 d\vec{r}_2 v^s(r_{12})^2\{u^s(\vec{r}_1,\ell)u^s(\vec{r}_2,\ell) - u^s(r_1)u^s(r_2)\}$$

$$= -\gamma_1 L^2$$

$$\gamma_1 = \frac{-a^2\alpha^4}{12(\alpha^2-1)^3}\{(\alpha^2+1)\ell n(\frac{3}{2+\alpha}) + \frac{(\alpha^2-1)(2\alpha+1)}{3(\alpha+2)}\}. \qquad (1.2.17)$$

The term in the second bracket in Eq.(1.2.16) may be reduced to a one dimensional integral by first integrating over $\vec{r}_1$,

$$\frac{\rho^2\beta^3}{2}\int d\vec{r}_1 d\vec{r}_2\, v^s(r_{12})^2\,\{u^s(\vec{r}_1,\ell)e^{-\beta u^s(\vec{r}_2,\ell)}\chi_2(\ell)$$

$$- u^s(r_1)e^{-\beta u^s(r_2)}\chi_2(0)\} = \left(\frac{3}{4\pi}\right)\int d\vec{x}_2\{[t(x_2) + iLp(x_2)\cos\theta_2]$$

$$\times e^{s(x_2)}(e^{-\beta w(x_2)}e^{iLG(x_2)\cos\theta_2} - e^{iLq(x_2)\cos\theta_2})$$

$$- t(x_2)e^{s(x_2)}\chi_2(0)\} = 3\int_0^\infty dx x^2\{t(x)[e^{F(x)}\left(\frac{\sin[LG(x)]}{LG(x)} - 1\right)$$

$$- e^{s(x)}\left(\frac{\sin[Lq(x)]}{Lq(x)} - 1\right)]$$

$$- Lp(x)[e^{F(x)}j_1(LG(x)) - e^{s(x)}j_1(Lq(x))]\}. \qquad (1.2.18)$$

The functions t(x) and p(x) are evaluated in Appendix D,

$$t(x) \equiv \frac{-a^5}{36x}\left(\frac{\alpha^2}{\alpha^2-1}\right)[e^{ax}E_1(3ax) + e^{ax}\{\ell n3 - E_1(ax)\}$$

$$- \frac{e^{a\alpha x}}{\alpha}E_1\{(2+\alpha)ax\} - \frac{e^{-a\alpha x}}{\alpha}\{\ell n\left(\frac{2+\alpha}{2-\alpha}\right) - E_1\{(2-\alpha)ax\}\}] \qquad (1.2.19)$$

and

$$p(x) \equiv x^{-1}[\frac{-a^4}{12}\left(\frac{\alpha^2}{\alpha^2-1}\right)\{e^{ax}E_1(3ax) - e^{-ax}\{\ell n3 - E_1(ax)\}$$

$$- e^{a\alpha x}E_1\{(2+\alpha)ax\}$$

$$+ e^{-a\alpha x}\{\ell n\left(\frac{2+\alpha}{2-\alpha}\right) - E_1\{(2-\alpha)ax\}\}) - \frac{3t(x)}{a^2}]. \qquad (1.2.20)$$

Eqs.(1.2.19) and (1.2.20) are only valid for values of α less than 2. The function E_1 is the exponential integral

$$E_1(y) \equiv \int_y^\infty dz \frac{e^{-z}}{z} \quad \text{for } y > 0. \tag{1.2.21}$$

Combining Eqs.(1.2.9), (1.2.10) and (1.2.16) we have

$$I_2(\ell) = I_2^{(1)}(\ell) + I_2^{(2,1)}(\ell) + I_2^{(2,2)}(\ell) \tag{1.2.22}$$

Thus,

$$T(\ell) \approx \exp\{-\gamma' L^2 + I_1(\ell) + I_2(\ell)\} \tag{1.2.23}$$

with $\gamma' = \gamma + \gamma_1$ and $I_1(\ell)$ is given by Eq.(1.2.7) and $I_2(\ell)$ by Eq.(1.2.20). The result in Eq.(1.2.22) is used in Eq.(1.1.4) to calculate $P(\varepsilon)$ at a singly charged point in the next section.

I.3 Results

The first step in using and evaluating the present theory is to determine the parameter α. In principle the expression for $T(\ell)$ in Eq.(1.1.24) is independent of the choice of α. However, in a practical calculation the infinite series appearing in the exponent of Eq.(1.1.24) is terminated and $T(\ell)$ is then no longer independent of the value of α. The procedure for selecting α is discussed in detail in I. Briefly, it involves finding a distinct and extended range of α values over which the $T(\ell)$ curve, hence the $P(\varepsilon)$ curve, remains stationary. In the stability region, or α-plateau, the second term in the series is small and the series rapidly converges.

A justification for the α selection procedure follows. For a given $\underline{a}$, a particular choice of α determines how much of the central interaction is treated by a Debye-chain or by a virial-expansion. The validity and speed of convergence of such expansions depend on the detailed nature of the interactions treated. A best choice of α will be that which splits the central interactions so as to optimize both expansions, thus giving a rapid convergence of Eq.(1.1.24). Then, a small variation of α about the best value should not significantly affect the results provided sufficient terms are retained in the infinite series.

Using this procedure we calculate $P(\varepsilon)$ curves and compare them with the results of I. Figures (1.5) and (1.6) show $P(\varepsilon)$ curves for $\underline{a}$ = 1.73 and $\underline{a}$ = 2.45, respectively. From the plots it can be seen that the corrections slightly lower and shift the peaks of the $P(\varepsilon)$ curves to higher ε values. Although not shown here, the contribution from these corrections become smaller with decreasing values of $\underline{a}$. In Figure (1.5) we compare our curves with Monte Carlo results[15] and in Figure (1.6) with Molecular Dynamic results.[16] The agreement for $\underline{a}$ = 1.73 is quite good. In this case, there exists a well defined α-plateau. For $\underline{a}$ = 2.45 the α-plateau reduces to the point where the existence of a plateau is in question; further, our results are not in agreement with the computer experiments. The lack of agreement, together with our earlier discussion of the α selection procedure would indicate the need to retain more terms in the series of Eq.(1.1.24) for $\underline{a} \gtrsim 2.0$.

I.4 Conclusion

We have shown that the previously developed collective coordinate approach to microfield distributions is equivalent to a hybrid

virial/Debye expansion. The two expansions are not independent; the long-range collective effects of the Debye-chains modify the short-range virial expansion. Hence, the range of validity of this formalism, when applied to systems where particles interact through long-range potentials, exceeds that of theories that use either expansion separately. The hybrid virial/Debye expansion formalism can easily be extended to the low-frequency microfield distributions in a plasma containing multiply charged ions.[7]

Numerical calculations of $P(\varepsilon)$ curves including some corrections neglected in I are presented in graphical form. These corrections correspond to correlations between the collective coordinates. Their contribution can be shown to be equivalent to keeping the next term in the Gram Charlier expansion of the Jacobian of the transformation to collective coordinates. Even though the effect of the corrections is small, for $\underline{a} = 2.45$ they improve agreement with the results of computer experiment.

In Eq.(1.1.22) we have ordered the terms in the sum by number of particles in a cluster. We now propose a different ordering based on the splitting of the central interactions. This split separates the central interaction into a strong short-ranged and a weak long-range contribution. The long-range weakly coupled part requires a Debye-chain expansion since these infinite range interactions give rise to collective effects. The strongly coupled part given by the χ-bonds and the effective interactions resulting from the summation of Debye-chains we treated in a virial expansion. However, instead we may identify a cluster by the number of χ-bonds it contains, and by the complexity[11] of the weakly coupled contributions. For example, the lowest order terms

in complexity are the ring graphs,[11] and the simple chains in Fig. (1.3). Systematic correction procedures in Refs. 17-20 discuss at length the summation of graphs of higher order in complexity. Therefore, we propose to order the terms in Eq.(1.1.24) by the two parameters: χ-bonds and complexity of the weakly coupled interactions.

In the preceding discussion we have implicitly assumed that the noncentral interactions constitute a weakly coupled system. This, of course, is only true for value of $\underline{a} \ll 2.0$. However, our original conjecture is that the microfield distribution is not very sensitive to the noncentral interactions. In this sense the noncentral interactions can be weakly coupled to the zeroth particle.

From Fig. (1.4) we see that in this new ordering scheme the graphs in (b2) and (c2) are of zeroth and first order in the strong coupling parameter, the number of χ-bonds. These graphs are higher order in complexity of the weakly coupled contributions than the graphs in (a), (b1), and (c1). We see that the graphs in (b2) and (c2) of zeroth and first order in χ-bonds are to be grouped with the ring graphs in (a) and the graphs in (b1), respectively.

From our results in Sect. I.3, we believe that by including terms containing three χ-bonds and lowest order in complexity in the Debye-chains we can extend the validity of our results to values of $a \gtrsim 2.0$.

Fig. 1.5 A comparison of $P(\varepsilon)$ curves for a = 1.732. The unmodified curve refers to the results of I. The modified curve includes the corrections in Sect. III. ε is in units of ε_o.

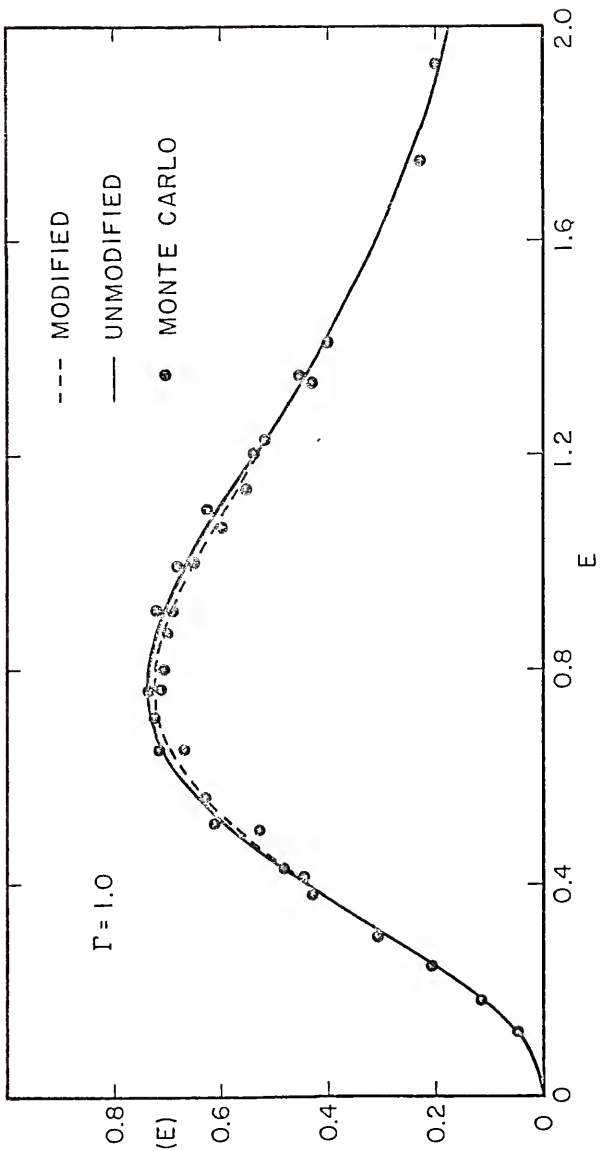
--- MODIFIED
— UNMODIFIED
MONTE CARLO
Γ= 1.0
P(E)
E
0
0.2
0.4
0.6
0.8
0.4
0.8
1.2
1.6
2.0

Fig. 1.6 A comparison of $P(\varepsilon)$ curves for $a = 2.45$. The unmodified curve refers to the results of I. The modified curve includes the corrections in Sect. I.3. ε is in units of ε_o.

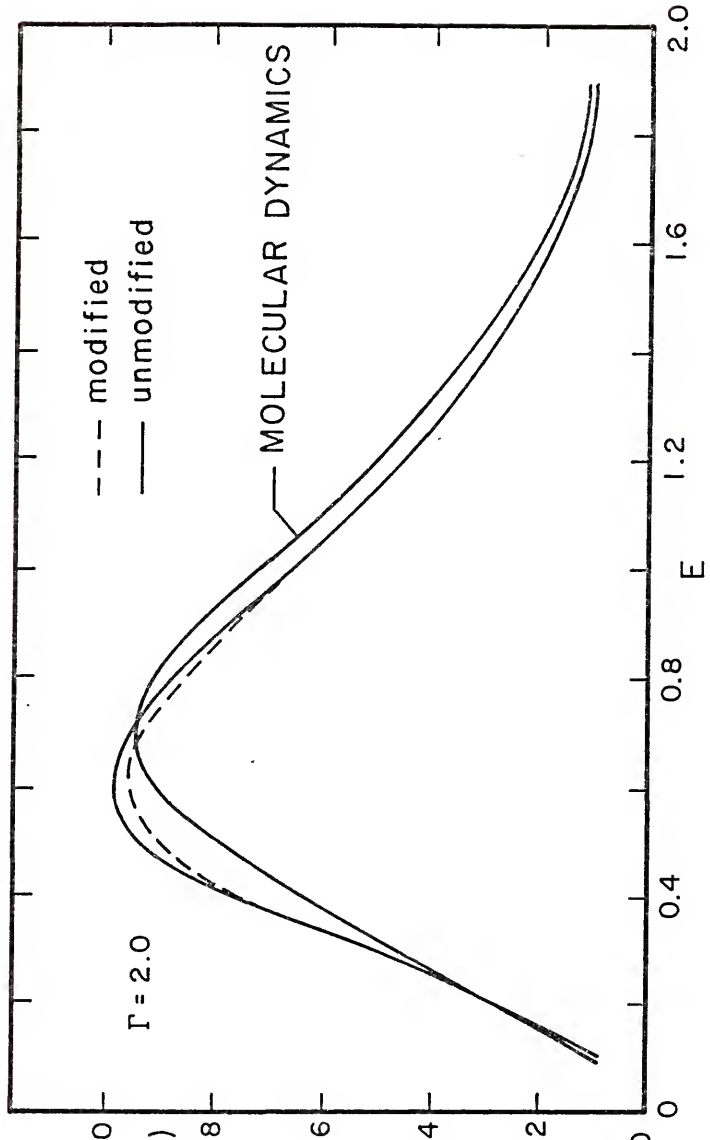
MOLECULAR DYNAMICS
modified
unmodified
Γ = 2.0
P(E)
E
0
0.2
0.4
0.6
0.8
1.0
0.4
0.8
1.2
1.6
2.0

CHAPTER II
LOW-FREQUENCY MICROFIELD

The spectral lines of radiating atoms or ions in a plasma are broadened due to the perturbation of the radiator by both the ions and the electrons of the plasma[21] (assuming for simplicity a two component plasma). Studies of the plasma broadened spectral lines have been quite successful in determining temperatures and densities for laboratory and astronomical plasmas.[22-25] In the past a number of fruitful results have been obtained in this area with the application of new methods developed in many-body physics and nonequilibrium statistical mechanics. Among these methods are propagator-operator equations,[26] Green's function techniques,[27] cluster expansions,[28] and formal kinetic theory of time correlation functions.[29] However, the problem of quantitatively predicting the line shape is difficult in general and is often simplified by reducing the calculation to one involving independent treatments of ion, electron, and radiator subsystems. Most past work has accomplished this under the following assumptions: (1) ions may be considered as static; (2) ion-electron interactions may be neglected and their effect partially accounted for by shielding the ion-ion interaction in an approximate fashion; and (3) electron-radiator interactions may be treated by perturbation theory. The first two assumptions allow the introduction of the low-frequency[3] microfield distribution which yields the Stark broadening due to the average static electron-shielded ion field. This is not a weak interaction effect and may not be

obtained by finite perturbation theory. The third assumption allows the electron "width and shift" operator[26] to be treated by perturbation theory. The ions and electrons are thus treated very differently in their interactions with the radiator, since the strong static effect and weak dynamic effect are two different approximations. In order for this description to be useful, the part of the line being described must be such that the radiation occurs in a time short compared to the time required for an ion to move significantly. On the other hand, the time of radiation must be long compared to corresponding times for electron motion since in finite perturbation theory the electron static effects are not treated properly. Fortunately, due to the large ratio of ion to electron mass, these conditions are often met over an interesting portion of the line.

The low-frequency microfield distributions are calculated by considering a gas of ions interacting through an effective screened potential. The ion electric fields are also assumed to be screened. The shielding in this calculation is a way to include electron screening effects, since the ion electric fields vary slowly overtimes on the order of the electron relaxation times. It is necessary for the conventional line-shape theories to treat the ions through low-frequency instead of high-frequency microfields, which contain no electron screening, in order to obtain agreement with experiments.

The purpose of this chapter is to show that the ad hoc introduction of the low-frequency microfields by the conventional theories leads to an incorrect expression of the electron width and shift operator. We demonstrate this point by two similar, but different approaches to the line-shape problem. The first approach takes advantage of the cluster

expansions developed in Chapter I in order to systematically obtain the electron screening of the ions in the microfield distribution. The second approach introduces an arbitrary static-ion field which must be defined at some point in the development. The ambiguity in the choice of the ion field is troublesome, but it allows us a freedom which is helpful in studying the dependence of the electron width and shift operator on the choice of microfield distribution. Both methods introduce the microfield distribution into the line-shape function without simultaneously introducing assumptions (1) and (2) above. It is then possible to neglect ion motion effects at the end of the development and compare with the conventinal theory results.

We will restrict our discussion to second-order theories which assume that the perturber-radiator interactions are weak and treat the width and shift operator to second order in these interactions. The second order theories are useful in laser produced plasma experiments[25] since the observed part of the line profiles from high-Z radiators is in the near wings, well inside the electron plasma frequency. Another reason for only discussing second-order theories is that the difficulties concerning the introduction of low-frequency microfields into the line-shape formalism are present in the second-order theories. Therefore, consideration of strong collisions, or so-called unified theories, is not necessary for the purpose in mind here.

II.1 Line Shape Function

The radiation spectrum of a quantum system is determined experimentally by measurement of the power radiated per unit time per unit frequency interval, averaged over the polarization and the

direction of radiation.[30,31] Since this quantity has been derived many times in a variety of ways, its derivation will not be included here. The power radiated when a particle makes a spontaneous dipole transition from one quantum state to another is,[31]

$$P(\omega) = (4\omega^4/3c^3) \sum_{i,f} |\langle i|\vec{d}|f\rangle|^2 \delta(\omega-\omega_{if}) W_i . \qquad (2.1.1)$$

In the above, $\langle i|\vec{d}|f\rangle$ represents the matrix elements for the radiator. The frequency, $\hbar\omega_{if}$, is the difference between the initial and final energies, E_i and E_f, of the entire radiator-plasma system; and W_i is the probability of occurence of the initial state in an ensemble. Eq.(2.1.1) may be manipulated to read as

$$P(\omega) = (4\omega^2/3c^3) I(\omega) \qquad (2.1.2)$$

where $I(\omega)$ is the line shape function defined by

$$I(\omega) = \pi^{-1} \mathrm{Re} \int_o^\infty dt\ e^{i\omega t} \mathrm{Tr}_{Rp}\{\rho_{Rp} \vec{d} \cdot \vec{d}(t)\} \qquad (2.1.3)$$

with (in units such that h=1)

$$\vec{d}(t) = e^{iHt}\ \vec{d}\ e^{-iHt} \qquad (2.1.4)$$

$$\rho_{Rp} = |i\rangle W_i \langle i| . \qquad (2.1.5)$$

Here, ρ_{Rp} is the equilibrium density matrix, H the total Hamiltonian, and Tr_{Rp} the trace over states of the radiator and plasma system. It

has been assumed from the outset that the momentum transferred to the radiator during the time of radiation is negligible, and therefore, that Doppler broadening due to the motion of the radiator is independent of the Stark broadening caused by the plasma.[32] It can be shown, under such conditions that the final line shape may be obtained by convoluting $I(\omega)$ with the Doppler profile.[33] In this situation, the operators appearing in Eq.(2.1.3) are dependent only upon the plasma degrees of freedom and the internal degrees of freedom of the radiator; there is no dependence on the center-of-mass variables of the radiator.

In a coordinate system with the origin at the radiator nucleus, the Hamiltonian may be written as

$$H = H_R + H_p + V_I \tag{2.1.6a}$$

where

H_R = Hamiltonian for the free radiator (no center-of-mass motion) (2.1.6b)

H_p = Hamiltonian for the plasma plus monopole term from the radiator-plasma interaction (2.1.6c)

V_I = radiator-perturber interaction (excluding monopole term already in H_p) (2.1.6d)

We have included the monopole part of the radiator-plasma interaction in H_p since in this frame it depends only on the plasma coordinates. The advantage in rearranging the Hamiltonian in this way is that the polarization of the plasma by the monopole part of the radiator-plasma interaction may be accounted for, while keeping the interaction V_I short

ranged. It should be noted that if Eq.(2.1.3) were to depend on the center-of-mass variables of the radiator, such a convenient separation would not be possible.

We now introduce two approximations present in most line broadening calculations. The radiator-perturber interaction V_I is replaced by a dipole interaction

$$V_I = V_{Re} + V_{Ri} \tag{2.1.7a}$$

with

$$V_{Re} \simeq \vec{d}\cdot\vec{E}_e \tag{2.1.7b}$$

$$V_{Ri} \simeq \vec{d}\cdot\vec{E}_i \tag{2.1.7c}$$

and $\vec{E}_e$ and $\vec{E}_i$ are the electron and ion electric fields, respectively. This replacement of the actual charge configuration by a dipole remains valid only if the contribution from interactions closer than a distance r_{min}, where the dipole approximation fails, are neglible. These conditions are satisfied for plasmas with densities such that the average interparticle distance is much greater than the size of the radiator.[34]

In the second approximation, we assume that the operator ρ_{Rp} can be factored in the manner

$$\rho_{Rp} \simeq \rho_R\rho_p. \tag{2.1.8}$$

This approximation neglects initial correlations of radiator and plasma due to V_I only, not to the monopole contribution included in H_p.

The factorization of ρ_{Rp} is a procedure which need not appear in the formal development of modern line shape broadening theories based on kinetic theory.[29,35,36] However, the factorization in these theories is sometimes made for computational convenience.[35]

The factorization in Eq.(2.1.8) allows us to express $I(\omega)$ in the form

$$I(\omega) = \pi^{-1} \text{ Re} \int_0^\infty dt \; e^{i\omega t} \langle \vec{d} \cdot \vec{D}(t) \rangle_R . \tag{2.1.9}$$

Here, Re stands for the real part and the brackets $\langle \quad \rangle_R$ indicate an average over only the radiator subsystem. The operator $\vec{D}(t)$ is the time developed radiator dipole operator, averaged over perturbers

$$\vec{D}(t) = \langle \vec{d}(t) \rangle_p \tag{2.1.10a}$$

$$\langle (\cdots) \rangle_p = \text{Tr}_p \rho_p (\cdots) \tag{2.1.10b}$$

The most general approaches to the theory of spectral line shapes have made use of either Green's functon[27] or Liouville operator[26] techniques. For the purpose here, the latter seems to be the most economical and transparent way to proceed.

The Liouville operator is defined by its action on an arbritary quantum mechanical operator.

$$Ly = i[H,y]; \tag{2.1.11}$$

that is, the Liouville operator gives the commutator with the Hamiltonian of the quantity on which it operates. Since

$$\frac{i\dot{\vec{d}}}{dt} = [\vec{d},H], \tag{2.1.12}$$

we have formally

$$\vec{d}(t) = e^{Lt}\,\vec{d}. \tag{2.1.13}$$

From the Hamiltonian given in Eq.(2.1.6), we have for the Liouville operator

$$L = L_0 + L_I, \tag{2.1.14a}$$

where

$$L_0 = L_R + L_p, \tag{2.1.14b}$$

$$L_R y = i[H_R,y], \tag{2.1.14c}$$

$$L_p y = i[H_p,y], \tag{2.1.14d}$$

$$L_I y = i[V_I,y]. \tag{2.1.14e}$$

The equation for the line shape can now be written in the form

$$I(\omega) = \langle \vec{d}\cdot\vec{D}(\omega)\rangle_R, \tag{2.1.15a}$$

with

$$\vec{D}(\omega) = \pi^{-1} \, \mathrm{Re} \int_0^\infty dt \; e^{i\omega t} \langle \vec{d}(t) \rangle_p$$

$$= -\pi^{-1} \, \mathrm{Im} \langle (\omega - iL)^{-1} \rangle_p \vec{d} \qquad (2.1.15b)$$

where the transform has been performed and Im stands for the imaginary part.

At this point the quasi-static ion approximation is introduced in conjunction with some approximation to account partially for the screening effect of electron-ion interactions.[31,32] We first approximate the Hamiltonian for the system,

$$H \simeq H_R + H_e + H_i^s + \vec{d} \cdot (\vec{E}_e + \vec{E}_i^s), \qquad (2.1.16a)$$

where

$$H_e = T_e + V_{ee} + \Phi_e \qquad (2.1.16b)$$

$$H_i^s = T_i + V_{ii}^s + \Phi_i^s. \qquad (2.1.16c)$$

In Eq.(2.1.16), T_e and T_i are the kinetic energy of the electrons and ions, respectively. The V_{ee} and V_{ii}^s are the electron-electron and ion-ion interactions, respectively; Φ_e and Φ_i^s the monopole radiator-electron and -ion interactions, respectively. The superscript ^{s} indicates that we consider the electron-ion interaction, V_{ei}, to produce some shielding effect on the ions. Henceforth, the explicit electron-ion interaction is dropped from the Hamiltonian. The shielding is frequently taken to be the Debye-Hückel[37] result. A similar identification follows for the electron- and shielded-ion-electric fields, $\vec{E}_e$ and $\vec{E}_i^s$. The subject of

the electron screening of the ion-ion interaction will be treated in greater detail later in this chapter and in the next.

Next, we assume that because of their large mass, the ion distribution is static. That is, it does not change significantly during the time of radiation,

$$i \frac{dH_i^s}{dt} = [H_i^s, H] \cong 0. \tag{2.1.17}$$

As a consequence of Eqs.(2.1.16) and (2.1.17) we arrive at the results

$$\vec{D}(t) = Tr_{i,e}\{\rho_i^s \rho_e \exp[(L_R + L_e + L_{Ri}^s + L_{Re})t]\vec{d}\}, \tag{2.1.18a}$$

where

$$\rho_e = \exp\{-\beta H_e\}/Z_e \text{ and } \rho_i^s = \exp\{-\beta H_i^s\}/Z_i^s, \tag{2.1.18b}$$

$$Z_e = Tr_e \exp\{-\beta H_e\} \text{ and } Z_i^s = Tr_i \exp\{-\beta H_i^s\}, \tag{2.1.18c}$$

$$L_{Ri}^s \, y = i[\vec{d} \cdot \vec{E}_i^s, y]. \tag{2.1.18d}$$

We can introduce the low-frequency ion microfield by inserting into the trace of Eq.(2.1.18a) a delta function $\delta(\vec{\varepsilon} - \vec{E}_i^s)$ along with an integral over the variable $\vec{\varepsilon}$. Then, because of the vanishing of the commutator in Eq. (2.1.17), we may everywhere replace $\vec{E}_i^s$ by $\vec{\varepsilon}$ with the result

$$\vec{D}(t) = \int d\vec{\varepsilon} \; Q_i^s(\vec{\varepsilon}) \, \langle \exp[(L_R(\vec{\varepsilon}) + L_e + L_{Re})t]\vec{d} \rangle_e. \tag{2.1.19}$$

Here the brackets $\langle \quad \rangle_e$ indicate an average over the electron subsystem, $L_R(\vec{\varepsilon})$ is the Liouville operator for the radiator in the external field $\vec{\varepsilon}$, and the static low-frequency ion microfield distribution is defined as

$$Q_i^s(\vec{\varepsilon}) = \langle \delta(\vec{\varepsilon} - \vec{E}_i^s) \rangle_i^s, \tag{2.1.20a}$$

where

$$\langle (\cdots) \rangle_i^s = \mathrm{Tr}_i \rho_i^s (\cdots). \tag{2.1.20b}$$

The result in Eq.(2.1.19) when substituted into the line shape expression, Eq.(2.1.19), provides the starting point for most line shape calculations,

$$I(\omega) = \int d\vec{\varepsilon}\; Q_i^s(\vec{\varepsilon}) J_e(\vec{\varepsilon},\omega), \tag{2.1.21a}$$

$$J_e(\vec{\varepsilon},\omega) = -\pi^{-1}\, \mathrm{Im} \langle \vec{d} \cdot [\omega - i(L_R(\vec{\varepsilon}) - L_e + L_{Re})]^{-1}\, \vec{d} \rangle_{R,e}. \tag{2.1.21b}$$

The expression for $J_e(\vec{\varepsilon},\omega)$ in Eq.(2.1.21) can be put in the form

$$J_e(\vec{\varepsilon},\omega) = -\pi^{-1}\, \mathrm{Im} \langle \vec{d} \cdot [\omega - iL_R(\vec{\varepsilon},\omega)]^{-1}\, \vec{d} \rangle_R, \tag{2.1.22}$$

where $L_R(\vec{\varepsilon},\omega)$, which can be interpreted as a frequency dependent, effective radiator Liouville operator, is amenable to perturbation theory.[31]

In this work we are interested in a second order theory; that is, we want an expression for $L_R(\vec{\varepsilon},\omega)$ which is second order in the radiator-perturber interaction, V_I. The procedure we follow is the same as that employed by Dufty.[38] First, we introduce the coupling constant λ,

$$L_I \rightarrow \lambda L_I, \tag{2.1.23}$$

which serves as our expansion parameter and will be set equal to one at the end of the calculation. Now, we make the definition,

$$\langle\{\omega - i[L_R + L_e + \lambda(L_{Re} + L_{Ri})]\}^{-1}\rangle_e = \{\omega - i[L_R + L_e + \lambda L_{Ri} + H(\lambda,w)]\}^{-1}, \tag{2.1.24}$$

where we have temporarily supressed the field dependence $\vec{\varepsilon}$. This expression formally defines the operator $H(\lambda,\omega)$, a function of radiator coordinates only, but implicitly contains broadening effects due to the electrons. We now assume the operator $H(\lambda,\omega)$ is analytic in λ, namely,

$$H(\lambda,\omega) = H^{(0)}(\omega) + \lambda H^{(1)}(\omega) + \lambda^2 H^{(2)}(\omega) + \cdots . \tag{2.1.25}$$

The next step involves expanding both sides of Eq.(2.1.24) and equating terms with like powers of λ to identify terms in the perturbation expansion of $H(\lambda,\omega)$. The left side of Eq.(2.1.24) may be expanded in a Lippmann-Schwinger expansion

$$\langle\{\omega - i[L_R + L_e + \lambda(L_{Re} + L_{Ri})]\}^{-1}\rangle_e = \langle R^0_{Re}(\omega)\rangle_e$$

$$+ i\lambda\langle R^0_{Re}(\omega) L_I R^0_{Re}(\omega)\rangle_e - \lambda^2\langle R^0_{Re}(\omega) L_I R^0_{Re}(\omega) L_I R^0_{Re}(\omega)\rangle_e$$

$$+ O(\lambda^3); \tag{2.1.26a}$$

$$R^0_{Re}(\omega) = [\omega - i(L_R + L_e)]^{-1}. \tag{2.1.26b}$$

If we use the identity

$$\langle L_e y(Re)\rangle_e = 0 \tag{2.1.27}$$

where y(Re) is an arbitrary function of the radiator and electron coordinates, Eq.(2.1.26) reduces to

$$\langle\{\omega - i[L_R + L_e + \lambda(L_{Re} + L_{Ri})]\}^{-1}\rangle_e + R^0_R(\omega)$$

$$+ i\lambda R^0_R(\omega)\langle L_I\rangle_e R^0_R(\omega) - \lambda^2 R^0_R(\omega)\langle L_I R^0_{Re}(\omega) L_I\rangle_e R^0_R(\omega)$$

$$+ O(\lambda^3), \tag{2.1.28a}$$

with

$$R^0_R(\omega) = [\omega - iL_R]^{-1}. \tag{2.1.28b}$$

The right hand side of Eq.(2.1.24) may be expanded in powers of λ using the operator identity,

$$\frac{\partial A^{-1}}{\partial \lambda} = -A^{-1}\frac{\partial A}{\partial \lambda}A^{-1}. \tag{2.1.29}$$

Then,

$$\{\omega - i[L_R + \lambda L_{Ri} + H(\lambda,\omega)]\}^{-1} = S_R^0(\omega) + i\lambda S_R^0(\omega)[L_{Ri} + H^{(1)}(\omega)]S_R^0(\omega)$$

$$-\lambda^2\{S_R^0(\omega)[L_{Ri} + H^{(1)}(\omega)]S_R^0(\omega)[L_{Ri} + H^{(1)}(\omega)]S_R^0(\omega)$$

$$-i\, S_R^0(\omega)H^{(2)}(\omega)S_R^0(\omega)\} + O(\lambda^3), \qquad (2.1.30a)$$

with

$$S_R^0(\omega) = \{\omega - i[L_R + H^{(0)}(\omega)]\}^{-1}. \qquad (2.1.30b)$$

Now by comparing Eqs.(2.1.28) and (2.1.30) we may identify $H^{(j)}(\omega)$ appearing in Eq.(2.1.25):

$$H^{(0)}(\omega) = 0 \qquad (2.1.31a)$$

$$H^{(1)}(\omega) = \langle L_{Re}\rangle_e \qquad (2.1.31b)$$

$$H^{(2)}(\omega) = i\{\langle L_{Re}R_{Re}^0(\omega)L_{Re}\rangle_e - \langle L_{Re}\rangle_e R_R^0(\omega)\langle L_{Re}\rangle_e\} \qquad (2.1.31c)$$

Before proceeding, we state that as a consequence of making the dipole approximation for the radiator-perturber interaction V_I, the average, $\langle L_{Re}\rangle_e$, in Eq.(2.1.31) vanishes:

$$\langle L_{Re}\rangle_e = 0. \qquad (2.1.32)$$

Retaining the lowest nonvanishing contribution, $H(\lambda,\omega)$ is given by

$$H(\omega) \equiv H^{(2)}(\omega) \simeq i\,\langle L_{Re}R_{Re}^0(\omega)L_{Re}\rangle_e. \qquad (2.1.33)$$

The final result for the line shape function then becomes

$$I(\omega) = \int d\vec{\varepsilon}\ Q_i^s(\vec{\varepsilon}) J_e(\vec{\varepsilon},\omega), \tag{2.1.34a}$$

where

$$J_e(\vec{\varepsilon},\omega) \simeq -\pi^{-1}\ \mathrm{Im} < \vec{d}\cdot\{\omega - iL_R(\vec{\varepsilon}) + \langle L_{Re} R_{Re}^0(\omega) L_{Re}\rangle_e\}^{-1}\ \vec{d}>_R . \tag{2.1.34b}$$

The essential feature of Eq.(2.1.34) is that the problem has been separated into two independent calculations. The broadening due to the ions is contained in $Q_i^s(\vec{\varepsilon})$, while $J_e(\vec{\varepsilon},\omega)$ contains the broadening due to the electrons. Since the range of the approximations used to obtain Eq.(2.1.34) are thoroughly discussed in the literature[30,31]; no further comments about them will be made here. Eq.(2.1.34) has been used by Hooper et al.[39,40] to calculate Stark broadened Lyman profiles from high-Z hydrogenic radiators immersed in hot dense plasmas encountered in a number of pellet-implosion experiments.[25]

II.2 Method I: Classical Plasmas

We return to the equation for the line shape function, Eq.(2.1.15),

$$I(\omega) = \langle \vec{d}\cdot\vec{D}(\omega)\rangle_R \tag{2.2.1a}$$

$$\vec{D}(\omega) = -\pi^{-1}\ \mathrm{Im}\langle[\omega - iL]^{-1}\rangle_p . \tag{2.2.1b}$$

We wish to express the line shape in the form,

$$I(\omega) = \int d\vec{\varepsilon}\ Q(\vec{\varepsilon})J(\vec{\varepsilon},\omega), \tag{2.2.2}$$

without assumptions (1) and (2).

To obtain the form of Eq.(2.2.2) for the line shape we follow Dufty.[38] There a method for introducing static microfield distributions was developed without neglecting electron-ion interactions or assuming static ions. Our development will closely follow that of Dufty.[38]

Make the following definition

$$\langle[\omega-iL]^{-1}\rangle_p \equiv \langle\{\omega-i[L_R + L_I + H_I(\omega)]\}^{-1}\rangle_p. \tag{2.2.3}$$

This expression formally defines the operator $H_I(\omega)$: $H_I(\omega)$ is a function of radiator coordinates only, but contains implicit broadening effects due to both ions and electrons. The Liouville operator L_I is defined in Eq.(2.1.14e). With the definition in Eq.(2.2.3), it is now possible to introduce a microfield function.

Consider the right hand side of Eq.(2.2.3)

$$\begin{aligned}
&\langle\{\omega-i[L_R + L_I + H_I(\omega)]\}^{-1}\rangle_p \\
&\quad = \int d\vec{\varepsilon}\ \langle\delta(\vec{\varepsilon}-\vec{E}_e-\vec{E}_i)\{\omega-i[L_R+ L_I+ H_I(\omega)]\}^{-1}\rangle_p \\
&\quad = \int d\vec{\varepsilon}\ \langle\delta(\vec{\varepsilon}-\vec{E}_e-\vec{E}_i)\{\omega-i[L_R+ L_I(\vec{\varepsilon}) + H_I(\omega)]\}^{-1}\rangle_p \\
&\quad = \int d\vec{\varepsilon}\ \langle\delta(\vec{\varepsilon}-\vec{E}_e-\vec{E}_i)\rangle_p\{\omega-i[L_R+ L_I(\vec{\varepsilon}) + H_I(\omega)]\}^{-1}.
\end{aligned} \tag{2.2.4}$$

Here, $L_I(\vec{\varepsilon})$ is obtained by replacing $\vec{E}_e+\vec{E}_i$ by $\vec{\varepsilon}$. The results in

Eq.(2.2.4) follow from the fact that the ion microfield commutes with everything in L_R and $H_I(\omega)$. Substitution of Eq.(2.2.4) into Eq.(2.2.1) yields

$$I(\omega) = \int d\vec{\varepsilon}\ \langle\delta(\vec{\varepsilon}-\vec{E}_e-\vec{E}_i)\rangle_p\ J_I(\vec{\varepsilon},\omega) \tag{2.2.5a}$$

$$J_I(\vec{\varepsilon},\omega) = -\pi^{-1}\ \mathrm{Im}\ \langle\vec{d}\cdot\{\omega-i[L_R(\vec{\varepsilon}) + H_I(\omega)]\}^{-1}\ \vec{d}\rangle_R. \tag{2.2.5b}$$

The expressions in Eq.(2.2.5) are formally similar to those in Eqs.(2.1.21) and (2.1.22) by construction. However, Eq.(2.2.5) follows from Eq.(2.2.1) without approximation. We remark that the ensemble average in the ion microfield distribution is over the entire plasma.

In order to determine $H_I(\omega)$, we use the same method discussed in obtaining a perturbation expansion for $H(\lambda,\omega)$. Then, to second order in radiator-perturber interaction,

$$H_I(\omega) \simeq H_I^{(2)}(\omega) = i\{\langle L_I(\omega-iL_o)^{-1}L_I\rangle_p - \langle L_I(\omega-L_R)^{-1}L_I\rangle_p\}, \tag{2.2.6}$$

where use has been made of the fact that

$$\langle L_I\rangle_p = 0. \tag{2.2.7}$$

With Eq.(2.2.6) we may write

$$I(\omega) = \int d\vec{\varepsilon}\ Q_I(\vec{\varepsilon})\ J_I(\vec{\varepsilon},\omega), \tag{2.2.8a}$$

where

$$J_I(\vec{\varepsilon},\omega) = -\pi^{-1}\ \mathrm{Im}\langle\vec{d}\cdot\{\omega - i[L_R(\vec{\varepsilon}) + \langle L_I(\omega - iL_o)^{-1}\ L_I\rangle_p$$

$$- \langle L_I(\omega - L_R)^{-1} L_I\rangle_p\}^{-1}\ \vec{d}\rangle_R, \qquad (2.2.8b)$$

and

$$Q_I(\vec{\varepsilon}) = \langle\delta(\vec{\varepsilon} - \vec{E}_e - \vec{E}_i)\rangle_p. \qquad (2.2.8c)$$

The result in Eq.(2.2.8) is formally similar to the previous result in Eq.(2.1.34). However, ion motion as well as electron motion is accounted for in the term,

$$\langle L_I(\omega - iL_o)^{-1} L_I\rangle_p, \qquad (2.2.9)$$

and the ensemble averages are now over the entire plasma with no assumptions about the ion-electron interactions. It will appear that the subtracted term in Eq.(2.2.6) removes the static part accounted for in the microfield function from $H_I(\omega)$.

II.3 Evaluation of $Q_I(\vec{\varepsilon})$

The result in Eq.(2.2.8) are equally applicable to a degenerate or classical plasma. In this section we assume a classical picture for the plasma, and find that the evaluation of the microfield distribution function is simplified.

As in Chapter I, we write for an isotropic plasma

$$P_I(\varepsilon) = (2\varepsilon/\pi)\int_o^\infty d\ell\ \ell\ \sin(\varepsilon\ell)T_I(\ell) \qquad (2.3.1a)$$

where

$$P_I(\varepsilon)d\varepsilon = 4\pi\varepsilon^2 Q_I(\varepsilon)d\varepsilon \tag{2.3.1b}$$

and

$$T_I(\ell) = Z_p(\ell)/Z_p \tag{2.3.2}$$

$$Z_p(\ell) = \int d\vec{R}_0 d\vec{R}_1 \cdots d\vec{R}_{N_i} d\vec{r}_1 \cdots d\vec{r}_{N_e} \exp\{-\beta V(\ell)\}. \tag{2.3.3}$$

We have adopted the capitalization convention where, for example, $\vec{R}_J$ denotes ion coordinates including the zeroth particle and $\vec{r}_j$ denotes electron coordinates. $V(\ell)$ is the "potential" of the system

$$V(\ell) = \{1 - i(\beta\chi e)^{-1} \vec{\ell}\cdot\vec{V}_o\}V \tag{2.3.4}$$

where χe is the electric charge of the zeroth particle and V the sum of Coulomb interactions between pairs of particles,

$$V = \sum_{1=i<j}^{N_e} v_{ee}(|\vec{r}_i - \vec{r}_j|) + \sum_{0=I<J}^{N_i} v_{ii}[|\vec{R}_I - \vec{R}_J|)$$

$$+ \sum_{I=0}^{N_i} \sum_{j=1}^{N_e} v_{ie}(|\vec{R}_I - \vec{r}_j|). \tag{2.3.5}$$

The formalism developed in Chapter I is easily extended to the two component plasma. The evaluation of $Z_p(\ell)$ in Eq.(2.3.3) leads to results similar to those in Eqs.(1.1.12) through (1.1.16) with one modification: the clusters may now contain electrons. This is easily accomplished by rewriting Eq.(1.1.13),

$$J = \text{set of } J = J_o + J_e + J_i \text{ particles} \tag{2.3.6a}$$

$$\mathbf{J!} = J_o!\, J_e!\, J_i! \tag{2.3.6b}$$

$$\mathbf{n}^{\mathbf{J}} = n_o^{J_o}\, n_e^{J_e}\, n_i^{J_i} \tag{2.3.6c}$$

where n_o, n_e, n_i, and J_o, J_e, J_i are the density and number of zeroth particle, ions, and electrons in an n-particle cluster, respectively.

As in Chapter I, the clusters not containing the zeroth particle exactly cancel in the expression for $T_I(\ell)$,

$$T_I(\ell) = \exp\{\Omega[A_2(\rho,\ell) - A_2(\rho,0)]\}. \tag{2.3.7}$$

The graphical representation for A_2 in Eq.(2.3.7) is topologically similar to the graphs representing A_2 in Eq.(1.1.16). The difference is that we replace the black vertices with black circles for the ions and black boxes for electrons. Some examples of the graphs are given in Fig.(2.1).

The next step requires some motivation. We wish to express the line shape function in a form similar to that in Eq.(2.1.34). That is, we wish to treat most of the ion broadening through an electron screened ion microfield ditribution without ignoring ion motion. Hence we will shield the ions in $Q_I(\vec{\varepsilon})$ and at the same time remove the explicit electron broadening from $Q_I(\vec{\varepsilon})$, transfering it into $J_I(\vec{\varepsilon},\omega)$, where it may be treated by perturbation theory.

First, we observe that it is possible to separate the clusters appearing in A_2 into two subclasses:

(2a) clusters containing no ions except the zeroth particle.

(2b) clusters containing the zeroth particle plus at least one other ion.

The sum of clusters in subclass (2a) gives the electron microfield distribution if there were no ions. For the subclass (2b) clusters we use a seminodal expansion which is similar to the nodal expansions of Abe[41], Meeron[42], Friedman[43], and Buckholtz.[44] Each subclass of (2b) graph is to be decomposed into a collection of graphs, each having potential- instead of f-Mayer bonds. The expansion is based on the definition of the f-functions,

$$f = \{\exp(-\beta v) - 1\} = \sum_{j=0}^{\infty} \{-\beta v\}^j/j! \ . \qquad (2.3.8)$$

A graphical representation of the decomposition is given in Fig.(2.2a) where n dashed lines connecting two vertices represent the factor $(-\beta v)^j/j!$ In Fig.(2.2a) the two vertices are arbritary; each may represent a radiator, ion, or electron.

The formidable number of clusters generated in the decomposition above, allows for a simplification which involves summing all simple electron chains.[11] There are five cases which are shown schematically in Fig.(2.2b). The wiggly lines represent the screened interactions between the two vertices in the figure. The possibilities for the pairs of vertices in Fig.(2.2b) are radiator-ion, radiator-electron, ion-ion, ion-electron,and electron-electron. It is understood that the two vertices at the endpoints of Fig.(2.2b) are part of a more complicated graph. We are summing all terms for which the graphs are the same except for the one sum of interactions represented. The intermediate electrons in Fig.(2.2b) do not interact with any particles except as explicitly shown in the figure.

Fig. 2.1 Graphical representation of A_2 for a plasma of ions and electrons. A black circle represents one of the N_i ions, a black box an electron, and a white circle the zeroth particle. The heavy solid lines represent f-Mayer functions.

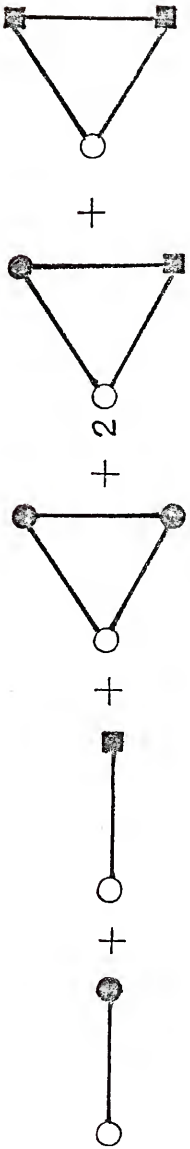

Fig. 2.2 The black circles represent any particle in the system, and the black boxes represent electrons only. (a) The decomposition of a f-Mayer bond into powers of $-\beta v$-bonds. (b) The effective interactions represented by a wiggly line is defined by sums of simple chains of electrons.

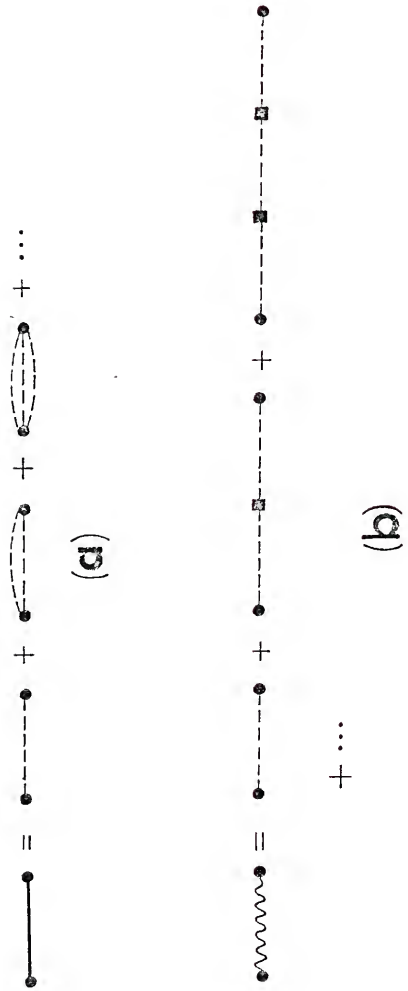

The screened interactions can be evaluated by introducing the Fourier transforms as in Appendix A. The effect of the screening is to introduce the dielectric function,

$$\varepsilon_e(q) = 1 + \rho_e \beta v_{ee}(q) \tag{2.3.9a}$$

$$v_{ee}(q) = 4\pi e^2/q^2. \tag{2.3.9b}$$

Hence we find that

$$-\beta v^s_{\sigma_1\sigma_2}(q) = -\beta v_{\sigma_1\sigma_2}(q)/\varepsilon_e(q);\ \sigma_1,\sigma_2 = i,e. \tag{2.3.10}$$

We have produced an expansion where at least three interaction bonds are connected to every electron vertex. Such vertices were defined in Ref. 41-44 as a node, hence the name nodal expansion has been adopted. In our case, an ion need only be twice connected. Therefore, we have developed a nodal expansion for only one species, or a seminodal expansion.[44]

If we neglect all subclass (2b) graphs containing one or more electron nodes, we find that the remaining graphs contain only ions interacting through a screened Coulomb potential. The screening of the bare ion-ion interacions is due to the electons and it is given by the Debye-Hückel result.

With this approximation, the subclass of (2b) graphs can be interpreted as a shielded ion microfield distribution. Furthermore, the electron microfield distribution and the shielded-ion microfield distribution are statistically independent,

$$\langle \delta(\vec{\varepsilon} - \vec{E}_e - \vec{E}_i) \rangle_p = \mathrm{Tr}_p \rho_p \delta(\vec{\varepsilon} - \vec{E}_e - \vec{E}_i)$$

$$\simeq \mathrm{Tr}_i \rho_i^s \, \mathrm{Tr}_e \rho_e \delta(\vec{\varepsilon} - \vec{E}_e - \vec{E}_i^s)$$

$$= \int d\vec{\varepsilon}' \{\mathrm{Tr}_i \rho_i^s \delta(\vec{\varepsilon}' - \vec{E}_i^s)\} \{\mathrm{Tr}_e \rho_e \delta(\vec{\varepsilon} - \vec{\varepsilon}' - \vec{E}_e)\} \qquad (2.3.11)$$

where ρ_e and ρ_i^s are defined in Eq.(2.1.18) with V_{ii}^s the sum of the Debye screened ion-ion interactions.

Substituting Eq.(2.3.11) into Eq.(2.2.8) yields

$$I(\omega) = -\pi^{-1} \, \mathrm{Im} \int d\vec{\varepsilon} d\vec{\varepsilon}' \, Q_i^s(\vec{\varepsilon}') \, \langle \delta(\vec{\varepsilon} - \vec{\varepsilon}' - \vec{E}_e) \rangle_e$$

$$\times \langle \vec{d} \cdot \{\omega - i[L_R(\vec{\varepsilon}) + H_I^{(2)}(\omega)]\}^{-1} \vec{d} \rangle_R$$

$$= -\pi^{-1} \, \mathrm{Im} \int d\vec{\varepsilon} \, Q_i^s(\vec{\varepsilon}) \, \langle \vec{d} \cdot \{\omega - i[L_R(\vec{\varepsilon}) + L_{Re} + H_I^{(2)}(\omega)]\}^{-1} \vec{d} \rangle_{R,e} . \qquad (2.3.12)$$

We can further manipulate Eq.(2.3.12) by introducing the projection operator P_e defined as

$$P_e y = \mathrm{Tr}_e \rho_e y. \qquad (2.3.13)$$

Then, using Zwanzig's projection operator techniques[45-48] described in Appendix E, we get for Eq.(2.3.12), in a second order theory,

$$I(\omega) = -\pi^{-1} \, \mathrm{Im} \int d\vec{\varepsilon} \, Q_i^s(\vec{\varepsilon}) \, \langle \vec{d} \cdot \{\omega - i[L_R(\vec{\varepsilon}) + H^{(2)}(\omega)]$$

$$+ \langle L_{Re} (\omega - iL_R)^{-1} L_{Re} \rangle_e \}^{-1} \vec{d} \rangle_R , \qquad (2.3.14)$$

where we have used the following properties of the projection operator

$$P_e L_{Re} y(R) = 0, \tag{2.3.15a}$$

$$P_e^2 = P_e, \tag{2.3.15b}$$

and

$$P_e\{L_R(\vec{\varepsilon}) + H_I^{(2)}(\omega)\}y(R) = \{L_R(\vec{\varepsilon}) + H_I^{(2)}(\omega)\}y(R). \tag{2.3.15c}$$

Here y(R) is an arbitrary function of the radiator coordinates.

The expression for the line shape given in Eq.(2.3.14) is of the form in Eq.(2.2.2), but is only applicable to classical plasmas. In addition, in getting to Eq.(2.3.14) we approximated $Q_I(\vec{\varepsilon})$. In Section II.7 we show that this approximation leads to complications.

II.4 Method II

In Section II.3 the classical treatment of the plasma considerably simplified the evaluation of $Q_I(\vec{\varepsilon})$. In particular, the identity

$$\exp\{-\beta H_p\}\ \exp\{i\vec{k}\cdot(\vec{E}_e + \vec{E}_i)\} = \exp\{-\beta H_p + i\vec{k}\cdot(\vec{E}_e + \vec{E}_i)\} \tag{2.4.1}$$

holds true only in the classical limit. For the quantum case, Eq.(2.4.1) must be replaced by the Baker-Campbell-Hausdorf formula.[49] In order to avoid this complication, we make the definition,

$$\langle(\omega - iL)^{-1}\rangle_p \equiv \langle\{\omega - i[L_R + L_{Ri}^{\Sigma} + H_{\Sigma}(\omega)\}^{-1}\rangle_p. \tag{2.4.2}$$

This expression formally defines the operator $H_\Sigma(\omega)$, a function of radiator coordinates only, which contains broadening effects due to both ions and electrons. The Liouville operator L_{Ri}^{Σ} is defined as

$$L_{Ri}^{\Sigma}\, y = i[\vec{d} \cdot \vec{E}_i^{\Sigma},\, y] \tag{2.4.3}$$

where the ion field $\vec{E}_i^{\Sigma}$ is arbitrary except that it only depends on ion coordinates. Clearly, $H_\Sigma(\omega)$ will depend on the choice of $\vec{E}_i^{\Sigma}$. With the definition in Eq.(2.4.2), it is now possible to introduce a microfield distribution function and write for Eq.(2.1.15),

$$I(\omega) = \int d\vec{\varepsilon}\; Q_i^{\Sigma}(\vec{\varepsilon}) J^{\Sigma}(\vec{\varepsilon},\omega) \tag{2.4.4a}$$

$$J^{\Sigma}(\vec{\varepsilon},\omega) = -\pi^{-1}\, \mathrm{Im}\langle \vec{d} \cdot \{\omega - iL_R(\vec{\varepsilon}) - iH_\Sigma(\omega)\}^{-1}\, \vec{d}\rangle_R \tag{2.4.4b}$$

$$Q_i^{\Sigma}(\vec{\varepsilon}) = \mathrm{Tr}_p \rho_p\; \delta(\vec{\varepsilon} - \vec{E}_i^{\Sigma}). \tag{2.4.4c}$$

By construction the result in Eq.(2.4.4) is formally similar to those in Eqs. (2.1.34) and (2.3.14), but Eq.(2.4.4) follows from Eq.(2.1.15) without approximation.

In order to determine $H_\Sigma(\omega)$, we use the same method previously used to obtain $H_I(\omega)$. Then, to second order in V_I,

$$H_\Sigma(\omega) \simeq H_\Sigma^{(2)}(\omega) = i\{\langle L_I(\omega - iL_o)^{-1} L_I\rangle_p - \langle L_{Ri}^{\Sigma}(\omega - iL_R)^{-1} L_{Ri}^{\Sigma}\rangle_p\}. \tag{2.4.5}$$

Use has been made of the fact that

$$\langle L_{Ri} \rangle_p = \langle L^{\Sigma}_{Ri} \rangle_p = \langle L_{Re} \rangle_p = 0. \tag{2.4.6}$$

With Eq.(2.4.5), we may write for $I(\omega)$,

$$I(\omega) = -\pi^{-1} \mathrm{Im} \int d\vec{\varepsilon}\; Q^{\Sigma}_i(\vec{\varepsilon})\, \langle \vec{d} \cdot \{\omega - iL_R(\vec{\varepsilon}) + \langle L_I(\omega - iL_o)^{-1} L_I \rangle_p -$$

$$- \langle L^{\Sigma}_{Ri}(\omega - iL_R)^{-1}\, L^{\Sigma}_{Ri} \rangle_p \}^{-1}\, \vec{d} \rangle_R. \tag{2.4.7}$$

Ion motion, as well as electron motion, is accounted for in the term,

$$\langle L_I(\omega - iL_o)^{-1} L_I \rangle_p, \tag{2.4.8}$$

and the ensemble averages are over the entire plasma with no approximation on the electron-ion interaction. Note that the subtracted term in Eq.(2.4.5) removes from $H^{(2)}_I(\omega)$ the static part accounted for in the microfield function.

Although Eq.(2.4.8) is formally similar to Eq.(2.3.14), there are two important differences. The first is the arbitrary ion field $\vec{E}^{\Sigma}_i$. The second is the difference in the subtracted terms that appear in $H^{(2)}_I(\omega)$ and $H^{(2)}_{\Sigma}(\omega)$. In order to further discuss the differences, we must first select $\vec{E}^{\Sigma}_i$.

II.5 Evaluation of $\langle \delta(\vec{\varepsilon} - \vec{E}^{\Sigma}_i) \rangle_p$

It remains to determine the ion field $\vec{E}^{\Sigma}_i$. In principle, $I(\omega)$ is not dependent on a particular choice of $\vec{E}^{\Sigma}_i$. In practice, however, $I(\omega)$ is calculated in some approximation scheme and it is no longer independent on the choice of $\vec{E}^{\Sigma}_i$. A first and simplest selection for $\vec{E}^{\Sigma}_i$

might be the electric field due to a collection of point charges. However, since $\vec{E}_i^{\Sigma}$ is a static field it is expected that the fast moving electrons screen the ion static field. Therefore, a 'best' choice for $\vec{E}_i^{\Sigma}$ could be an electron shielded static ion field. This, of course, is an ad hoc method of selection. Below we propose a plausibility argument for selecting the field $\vec{E}_i^{\Sigma}$.

We start with the formal expression for the microfield distribution function

$$Q_i^{\Sigma}(\vec{\varepsilon}) = \langle \delta(\vec{\varepsilon} - \vec{E}_i^{\Sigma}) \rangle_p \tag{2.5.1}$$

which for an isotropic system[2], can be written,

$$P_{\Sigma}(\vec{\varepsilon}) = (2\varepsilon/\pi) \int_0^{\infty} d\ell \; \ell \sin(\varepsilon\ell) T_{\Sigma}(\ell) \tag{2.5.2a}$$

$$T_{\Sigma}(\vec{\varepsilon}) = \langle \exp\{ i\vec{\ell}\cdot\vec{E}_i^{\Sigma} \} \rangle_p . \tag{2.5.2b}$$

In Eq. (2.5.2) the ensemble average is over the entire plasma. But because the electric field $\vec{E}_i^{\Sigma}$ depends only on ion coordinates it is possible to formally perform the trace over the electrons:

$$\begin{aligned} \langle e^{i\vec{\ell}\cdot\vec{E}_i^{\Sigma}} \rangle_p &= \mathrm{Tr}_p \rho_p \, e^{i\vec{\ell}\cdot\vec{E}_i^{\Sigma}} \\ &= \mathrm{Tr}_i \{ \mathrm{Tr}_e \rho_p \} e^{i\vec{\ell}\cdot\vec{E}_i^{\Sigma}} \\ &= \mathrm{Tr}_i \rho_i^{\Sigma} \, e^{i\vec{\ell}\cdot\vec{E}_i^{\Sigma}} \\ &= \langle e^{i\vec{\ell}\cdot\vec{E}_i^{\Sigma}} \rangle_i^{\Sigma} \end{aligned} \tag{2.5.3}$$

which defines the brackets $\langle \quad \rangle_i^{\Sigma}$ and ρ_i^{Σ}, an effective ion density operator.

In order to make further progress with the operator ρ_i^{Σ} we use the second quantized representation of the equilibrium reduced density operators,[50]

$$\langle \vec{R}_1,\ldots,\vec{R}_{N_i} | \rho_i^{\Sigma}(1,\ldots,N_i) | \vec{R}_1,\ldots,\vec{R}_{N_i} \rangle$$

$$= \langle \psi^+(\vec{R}_1)\ldots\psi^+(\vec{R}_{N_i})\psi(\vec{R}_{N_i})\ldots\psi(\vec{R}_1)\rangle_p . \qquad (2.5.4)$$

The operators, $\psi^+(\vec{R}_I)$ and $\psi(\vec{R}_I)$, are the ion creation and annihilation operators for the spatial point, $\vec{R}_I$. Now the N_i-particle Green's function is defined by

$$G(1,\ldots,N_i;1',\ldots,N_i') = -\langle T_\tau\{\psi(1)\ldots\psi(N_i)\psi^+(N_i')\ldots\psi(1')\}\rangle_p \qquad (2.5.5)$$

where T_τ orders the operators according to their value τ, with the smallest at the right. The operator T_τ also carries the signature $(-1)^P$, where P is the number of permutations of fermion operators needed to restore the original ordering. Therefore, Eq.(2.5.4) may be expressed as

$$\langle \vec{R}_1,\ldots,\vec{R}_{N_i} | \rho_i^{\Sigma}(1,\ldots,N_i) | \vec{R}_1,\ldots\vec{R}_{N_i} \rangle$$

$$= -G(1,\ldots,N_i;1^+,\ldots,N_i^+) \qquad \begin{matrix} \tau_{N_i} = \tau^+_{N_i-1} \\ \tau_{N_i-1} = \tau^+_{N_i-2} \\ \vdots \\ \tau_2 = \tau_1^+ \end{matrix} \qquad (2.5.6)$$

The plus signs used as superscripts are intended to serve as reminders of the particular infinitesimal τ ordering required to reproduce the orders of the factors in Eq.(2.5.4).

To evaluate the many-particle Green's function in Eq.(2.5.5) we may use Feynman-Dyson perturbation theory.[51] Each term in the perturbation expansion may be represented[51] by a Feynman diagram. This perturbation theory is an expansion in the bare interaction. However, due to the long range of the Coulomb interaction the expansion diverges term by term[51-54] and it is necessary to sum a selected class of diagrams, whose sum yields a finite contribution. After examining the perturbation expansion, the selected class of diagrams to be summed are the so-called ring diagrams,[51-54] which are the most divergent set of diagrams. This frequently used approximation in the theory of Coulomb systems is equivalent to the random phase approximation (RPA) of Bohm and Pines.[55]

In what follows, we will treat the electrons in the RPA. This approximation is most simply treated by introducing the effective two-body interaction defined in Fig.(2.3). This approximation to the effective interaction reduces in the classical limit to the Debye-Hückel result.[52,54] It is understood that the Green's functions at the endpoints of Fig.(2.3) are part of a more complicated diagram. We are summing all electron terms for which the diagrams are the same except for the sum represented. The intermediate electrons in Fig.(2.3) do not interact with any other particles except as explicitly shown in the figure. The resummation formally eliminates all the electrons from the diagrams and replaces the bare Coulomb ion-ion and ion-radiator interactions with effective potentials. Note that in this method the electrons do not shield the ion field $\vec{E}_1^{\Sigma}$, while in Method I the electrons do screen the bare ion field.

Fig. 2.3 The effective, temperature dependent ion-ion interaction is defined in terms of the electron proper polarization part π_e^o.

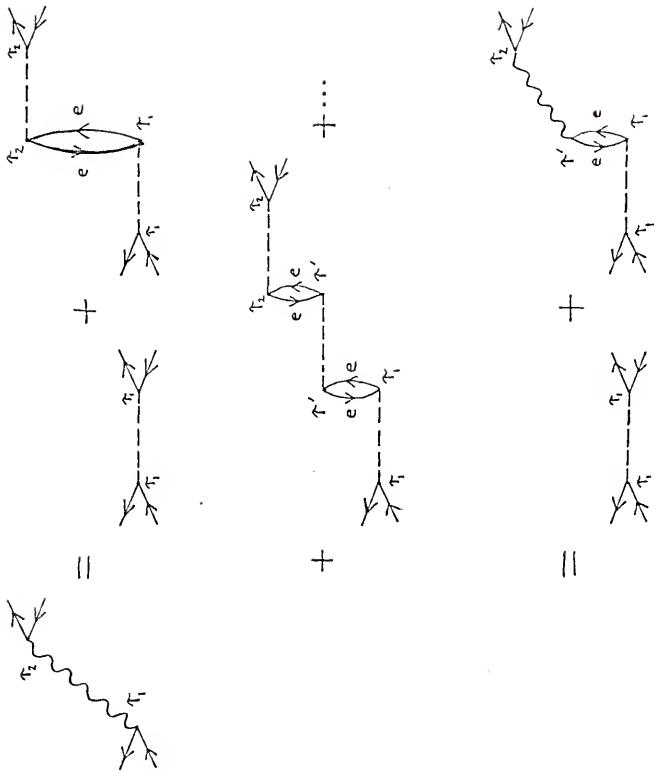
π₂
e
e'
π'
π₁
+
=
+
+ ...
=

The effective interactions may be expressed in terms of the electron proper polarization part,[52,53]

$$U_\tau^\Sigma = \sum_{0\le I<J} u^\Sigma(\vec{R}_I-\vec{R}_J;\tau) \tag{2.5.7a}$$

$$u^\Sigma(\vec{R}_I-\vec{R}_J;\tau) = [(2\pi)^3\beta]^{-1} \sum_{n=0}^{\infty} \int d\vec{q}\ \exp\{i\vec{q}\cdot(\vec{R}_I-R_J)-i\nu_n\tau\}u_{IJ}^\Sigma(\vec{q};\nu_n) \tag{2.5.7b}$$

$$\nu_n = 2\pi n/\beta \tag{2.5.7c}$$

where

$$u_{IJ}^\Sigma(\vec{q};\nu_n) = v_{IJ}(\vec{q})\{1 - v_{ee}(q)\pi_e^o(q,\nu_n)\}^{-1}. \tag{2.5.7d}$$

In Eq.(2.5.7) π_e^o is the random phase approximation to the electron proper polarization part, π_e^*, where π_e^* is defined[52,53] as the sum of all electron polarization parts that can not be separated into disconnected parts by cutting a single electron-electron interaction line.

Since the ion-ion and ion-radiator (monopole part) interactions have been screened by the electrons, it seems plausible to select $\vec{E}_i^\Sigma$ as follows,

$$\vec{E}_i^\Sigma = -\vec{\nabla}_o U_\tau^\Sigma. \tag{2.5.8}$$

This choice of $\vec{E}_i^\Sigma$ is certainly not unique and by no means has it been derived rigorously. Nevertheless, it seems plausible[3] that if the ion-radiator monopole term is screened by the electrons, then the electric field at the radiator due to the ions should also be screened. Again we emphasize that $\vec{E}_i^\Sigma$ is arbitrary and the choice given in Eq.(2.5.8)

involves some hindsight. This particular choice for $\tilde{E}_i^{\Sigma}$ will allow us to consider systematic corrections to the "conventional" line shape theories discussed in Sect. II.1. Finally we remark that the effective potential has been evaluated in the ring approximation, but systematic corrections are possible by including corrections[17-20,56,57] to π_e^o in Eq.(2.5.8d).

II.6 The Classical Limit

Consideration of the classical limit of an interacting quantum mechanical system by looking at a Green's function formulation, in that limit, has been discussed by Smith.[58] In Ref. 58, Smith starts with the usual Feynman rules[52] for evaluating diagrams and derives a set of rules which apply in the classical limit. Application of these rules to the diagrammatic expansion of the Green's function leads to the equation of state in the cluster form.

In the grand canonical ensemble, thermodynamic quantities[59] are functions of the volume Ω, the temperature T, and the chemical potential μ. For noninteracting bosons or fermions there are two length parameters, $\Omega^{1/3}$ and the thermal wavelength, Λ_σ, which for a particle of mass m_σ is defined as,

$$\Lambda_\sigma = [2\pi\beta/m_\sigma]^{1/2}. \tag{2.6.1}$$

In the classical limit we let the fugacity, $z_\sigma = e^{\beta\mu_\sigma}$, go to zero while the quotient $(z_\sigma/\Lambda_\sigma^3)$ remains finite and is in fact equal to the particle density.[58] For an interacting system the range of the potential, δ_o, is another length parameter and the classical limit is defined by $z_\sigma \to 0$

while $(z_\sigma \delta_o / \Lambda_\sigma^3)$ remains finite for nonzero δ_o. Terms of higher order in $(z_\sigma \delta_o / \Lambda_\sigma^3)$ will then be dropped. As a result, there are two basic simplifications over the quantum case. One is the restriction of diagrams that can contribute, and the other is the elimination of some terms in the free particle Green's function. The simplifications, summarized by Smith[58] in the forms of rules which apply in the classical limit, are stated here without proof:

(1) The only diagrams which contribute are those for which there is some τ ordering, such that, of all the free Green's functions in a loop, exactly one of them has $\tau<0$. The chain of propagators running between two fixed points may have either zero or one propagator with $\tau<0$, depending on whether the two fixed points are forward or backward in tau, with respect to each other. As a result of this rule, no interaction line can have both ends on the same loop.

(2) In any loop, all propagators with $\tau>0$ may be replaced by $-\delta(x)$ and the one propagator with $\tau<0$ by $\pm z_\sigma/\Lambda_\sigma^3$, the (+) for fermions and the (-) for bosons. This implies that all space coordinates of a given loop are the same.

Since in a coordinate representation only the diagonal elements are required for the reduced operator ρ_i^Σ in Eq.(2.5.5), the diagrams associated with the reduced distribution functions only involve closed loops of the radiator, ions, and electrons. In particular, the diagonal elements will have chains of propagators running from a fixed point, say $(\vec{x},\tau)$, back to the fixed point $(\vec{x},\tau^+)$. The propagator returning to $(\vec{x},\tau^+)$, thus, contributes a factor $\pm (z_\sigma/\Lambda_\sigma^3)$. This chain behaves now exactly as a loop. Rules (1) and (2) may now be used to evaluate ρ_i^Σ in the classical limit with the result,

$$\rho_i^{\Sigma} = \exp\{-\beta(T_i + V_{ii}^{s})\}/Tr_i \exp\{-\beta(T_i + V_{ii}^{s})\}, \qquad (2.6.2)$$

where V_{ii}^{s} is a screened ion-ion interaction where the screening, due to the electrons, is treated in a Debye-chain expansion. Therefore, in the classical limit $Q_i^{\Sigma}(\vec{\varepsilon})$ reduces to $Q_i^{s}(\vec{\varepsilon})$. However, in this limit Eq. (2.4.7) does not reduce to Eq.(2.3.14). The difference appears in the subtracted terms:

$$\langle L_{Ri}^{\Sigma}(\omega - iL_R)^{-1} L_{RI}^{\Sigma}\rangle_p \text{ in Eq. (2.4.7)}, \qquad (2.6.3a)$$

as compared to

$$\langle L_I(\omega - iL_o)^{-1}L_I\rangle_p - \langle L_{Re}(\omega - iL_R)^{-1}L_{Re}\rangle_e , \qquad (2.6.3b)$$

appearing in Eq. (2.3.14).

II.7 Comparison of the Methods

It is convenient to rewrite the results from the previous sections in order to compare them. First, for the conventional line shape formalism described in Section II.1, which assumes static ions and accounts for ion-electron correlations through a screening of the ion-ion interaction, we write

$$I(\omega) = -\pi^{-1}\mathrm{Im}\int d\vec{\varepsilon}\; Q_i^{s}(\vec{\varepsilon})\langle\vec{d}\cdot\{\omega - iL_R(\vec{\varepsilon}) +$$

$$+ \langle L_{Re}[\omega - i(L_R + L_e)]^{-1}L_{Re}\rangle_e\}^{-1}\vec{d}\rangle_R. \qquad (2.7.1)$$

The result of Method I, which takes advantage of a cluster expansion formulation of the microfield distribution in order to screen the ions, is given by

$$I(\omega) = -\pi^{-1}\mathrm{Im}\int d\vec{\varepsilon}\; Q_i^s(\vec{\varepsilon})\; \langle \vec{d}\cdot\{\omega - iL_R(\vec{\varepsilon}) + \langle L_I(\omega - iL_o)^{-1}L_I\rangle_p$$

$$- [\langle L_I(\omega - iL_R)^{-1}L_I\rangle_p - \langle L_{Re}(\omega - iL_R)^{-1}L_{Re}\rangle_e]\}^{-1}\vec{d}\rangle_R. \quad (2.7.2)$$

The second approach, Method II, introduces an arbitrary ion field. This field must then be chosen, and we have given plausibity arguments for our choice of $\vec{E}_i^{\Sigma}$. With this method, the resulting line-shape function is

$$I(\omega) = -\pi^{-1}\mathrm{Im}\int d\vec{\varepsilon}\; Q_i^{\Sigma}(\vec{\varepsilon})\; \langle \vec{d}\cdot\{\omega - iL_R(\vec{\varepsilon}) - \langle L_I(\omega - iL_o)^{-1}L_I\rangle_p$$

$$+ \langle L_{Ri}^{\Sigma}(\omega - iL_R)^{-1}\, L_{Ri}^{\Sigma}\rangle_p\}^{-1}\vec{d}\rangle_R. \quad (2.7.3)$$

Since Eq.(2.7.2) applies only to classical plasmas, we temporarily restrict our discussion to such plasmas. The effective interactions in $Q_i^s(\vec{\varepsilon})$ of Eq.(2.7.1) are usually taken to be the Debye-Hückel result, therefore, all three microfield distribution functions in Eqs.(2.7.1) through (2.7.3) are equal in the classical limit. As mentioned before, there are differences in the denominators appearing in the curly brackets of these equations. Obviously, Eq.(2.7.1) is not expected to agree with the other two equations since it contains assumptions (1) and (2); the neglect of ion motion and electron-ion correlations. At this time, it is instructive to make these two approximations in Eqs.(2.7.2)

and (2.7.3). Then, for the denominator in Eq.(2.7.2), $\{\cdots\}^{-1}$, we get

$$\{\omega - iL_R(\vec{\varepsilon}) + \langle L_I(\omega - iL_o)^{-1}L_I\rangle_p - [\langle L_I(\omega - iL_R)^{-1}L_I\rangle_p - \langle L_{Re}(\omega - iL_R)^{-1}L_{Re}\rangle_e]\}^{-1}$$

$$\rightarrow \{\omega - iL_R(\vec{\varepsilon}) + \langle L_{Re}[\omega - i(L_R + L_e)]^{-1}L_{Re}\rangle_e\}^{-1} \qquad (2.7.4)$$

and for the denominator in Eq.(2.7.3), $\{\cdots\}^{-1}$,

$$\{\omega - iL_R(\vec{\varepsilon}) + \langle L_I(\omega - iL_o)^{-1}L_I\rangle_p - \langle L^{\Sigma}_{Ri}(\omega - iL_R)^{-1}L^{\Sigma}_{Ri}\rangle_p\}^{-1}$$

$$\rightarrow \{\omega - iL_R(\vec{\varepsilon}) + \langle L_{Re}[\omega - i(L_R + L_e)]^{-1}L_{Re}\rangle_e\}^{-1} \qquad (2.7.5)$$

Notice that in Eq. (2.7.3) the ion field $\vec{E}^{\Sigma}_i$ is defined by Eq. (2.5.8), and is therefore dependent on the ion-electron interactions. Hence, $\vec{E}^{\Sigma}_i$ goes over to $\vec{E}_i$ when electron-ion interactions are neglected. Clearly, both methods reduce to Eq.(2.7.1) with these two approximations.

Let us relax the approximations immediately preceding Eq.(2.7.4) and examine Eq.(2.7.2) in more detail. As indicated in Section II.3, an infinite number of graphs were neglected in getting to Eq.(2.3.11). In particular, all subclass (2b) graphs containing one or more electron nodes were neglected. Some neglected graphs contain the corrections to the simple chains of electrons: corrections to the Debye-Hückel screening.[17-20] But more than corrections to the electron screening of the ions is neglected. For example, the ion screening of the electrons is not included. But in the left hand side of Eq.(2.7.4) the terms in brackets are subtracting from $\langle L_I(\omega - iL_o)^{-1}L_I\rangle_p$ the broadening already

included in the microfield. Therefore, for a consistent treatment of the line shape, we require that effects neglected in the microfield distribution, $Q_i^S(\vec{\varepsilon})$, must also be neglected in the left hand side of Eq.(2.7.4). As an example, consider two terms from Eq.(2.7.4)

$$\langle L_{Re}(\omega - iL_R)^{-1} L_{Re}\rangle_p - \langle L_{Re}(\omega - iL_R)^{-1} L_{Re}\rangle_e . \tag{2.7.6}$$

If we define

$$\rho_e^{eff} \equiv Tr_i \rho_p \tag{2.7.7}$$

then we may write for Eq.(2.7.6)

$$Tr_e\{\rho_e^{eff} - \rho_e\} L_{Re}(\omega - iL_R)^{-1} L_{Re} \simeq Tr_e\{\rho_e - \rho_e\} L_{Re}(\omega - iL_R)^{-1} L_{Re} = 0 \tag{2.7.8}$$

where we have neglected the ions screening in ρ_e^{eff}. For the remaining terms in Eq.(2.7.4) we should also be careful and neglect similar contributions. Certainly, this leads to a complicated evaluation of Eq.(2.7.2).

A similar complication does not occur in Eq.(2.7.3). The term containing L_{Ri}^{Σ} in Eq.(2.7.5) exactly subtracts from $\langle L_I(\omega - iL_o)^{-1} L_I\rangle_p$ the broadening effects in $Q_i^{\Sigma}(\vec{\varepsilon})$ (in a second order theory). For consistency all that is required is that the average over the plasma be evaluated identically in both terms. Also, the range of validity of Eq.(2.7.3) includes both quantum and classical plasmas. The difficulty with this approach is in justifying the selection of $\vec{E}_i^{\Sigma}$.

II.8 Summary

The two methods developed in the previous sections demonstrate the problems involved with introducing low-frequency microfields in the line-shape function. Even though the formal expressions for the line-shape function derived from Methods I and II are not identical, it is clear that both methods modify the expression for the electron width and shift operator appearing in the conventional theories. In fact, the different forms of the width and shift operators resulting from the two approaches, emphasizes that the formal expression for the width and shift operator is very much dependent on the choice of microfield distribution.

We have demonstrated that the modifications to the electron width and shift operator vanish if ion-electron correlations are neglected. However, this approximation 'overcounts' the electrons. That is, if we neglect ion-electron correlations in the width and shift operator and not in the microfield, then the implicit electron broadening in the low-frequency microfield is also included, to second order, in the width and shift operator. This, of course, is not a consistent approximation. In this dissertation we will not study these corrections to the electron broadening any further. Our intention is to simply point out the difficulties involved with an ad hoc treatment of the line-shape function.

In the next chapter we assume that the complications discussed above will be resolved by future research. Having taking this point of view, we will proceed to investigate quantum mechanical corrections to the electron screening of the ions in the calculation of low-frequency microfields.

CHAPTER III
QUANTUM CORRECTIONS TO THE LOW-FREQUENCY COMPONENT MICROFIELD DISTRIBUTION

The spectral line shapes for an atom or an ion radiating in a plasma are determined[21] by the interactions of the radiator with all of the components of the plasma. In relation to this problem, various theories of ion microfield distributions have been formulated.[2-6] In these theories, electric fields of two types are considered: a high-frequency and a low-frequency component. The distribution of the high-frequency component is calculated[3,5] by considering a gas of ions interacting through a Coulomb potential and immersed in a uniform neutralizing background. The distribution of the low-frequency component is determined[4,6] by considering a gas of ions interacting through an effective, screened potential. The shielding of the ions in the latter case is a way to include electron screening effects, since the ion electric fields vary slowly over times on the order of the electron relaxation times. The effective potential is chosen to be the Debye-Hückel result,[37] which applies to classical electrons and long times.

It is possible that the ions may be treated reasonably well with a classical picture, even when the density and temperature conditions require a quantum mechanical formulation of an electron gas. This dual behavior is due to the large ion-to-electron mass ratio. In this chapter we investigate such a situation and treat quantum mechanically the electron screening of classical ions.

III.1 Low-Frequency Microfield Distribution

The line shape function given by Eq.(2.7.1) involves the evaluation of the shielded, static ion distribution function

$$Q_i^s(\vec{\varepsilon}) = \mathrm{Tr}_i \rho_i^s \delta(\vec{\varepsilon} - \vec{E}_i^s) \tag{3.1.1}$$

The microfield distribution in Eq.(3.1.1) can be evaluated with the method developed in Chapter 1 with only simple modifications necessary in order to account for the effective potential.

As in Chapter 1, the problem is to determine the electric microfield distribution function $P(\vec{\varepsilon})$ at a point with charge χe, which is found from an evaluation of Eq.(1.1.4),

$$P(\varepsilon) = (2\varepsilon/\pi) \int_o^\infty d\ell \; \ell \; \sin(\varepsilon\ell) T(\ell), \tag{3.1.2}$$

where $T(\ell)$ is given by

$$T(\ell) = Z_N^{-1} \int \cdots \int d\vec{r}_o d\vec{r}_1 \cdots d\vec{r}_N \exp\{-\beta V_N + i(\chi e)^{-1} \vec{\ell} \cdot \vec{\nabla}_o V_N\}. \tag{3.1.3}$$

In Eq. (3.1.3) $\vec{r}_j$ represents the position of the j-th particle, $\beta=(kT)^{-1}$, and Z_N is the configurational partition function. The potential energy of the system, V , is expressed as,

$$V = \sum_{0=i<j} v_{ij}^s. \tag{3.1.4}$$

The two particle effective interaction, v_{ij}^s, is usually taken to be the

Debye-Hückel result,[4,6]

$$v_{ij}^{s}(r) = Z_i Z_j e^2 \exp\{-r/\lambda_e\}/r, \tag{3.1.5a}$$

where

$$Z_i = \begin{cases} \chi & i=0 \\ Z & i\neq 0 \end{cases}. \tag{3.1.5b}$$

Here, Ze is the charge of one ion and λ_e is the electron Debye length defined by,

$$\lambda_e = [4\pi e^2 \rho_e \beta]^{1/2}, \tag{3.1.6}$$

where ρ_e is the electron density. By requiring the total system to be neutral, the ion and electron densities are related by the expression,

$$\rho_i = Z\rho_e.$$

In what follows we assume the electrons to be quantum mechanical while still retaining a classical picture for the ions. With this assumption, the Debye-Hückel result of Eq.(3.1.5) is no longer valid.

III.2 Effective Quantum Interaction

In order to evaluate the effective quantum interaction, it is convenient to introduce the Fourier transform defined in Eq.(A-2), and the generalized dielectric function,[52]

$$\varepsilon_e(\vec{q},\nu_n) = 1 - v_{ee}(q)\pi_e^*(\vec{q},\nu_n), \tag{3.2.1}$$

where π_e^* is the proper polarization part[52] of the one component electron gas, and v_{ee} is the Fourier transform of the electron-electron Coulomb interaction:

$$v_{ee}(q) = 4\pi e^2/q^2. \tag{3.2.2}$$

In terms of the dielectric function the shielded interaction may be expressed as,[52]

$$u_{ij}^{\Sigma}(\vec{q},\nu_n) = v_{ij}(q)\varepsilon_e(q,\nu_n), \tag{3.2.3}$$

where $v_{ij}(q)$ is the Fourier transform of the bare Coulomb ion-ion interaction,

$$v_{ij}(q) = 4\pi Z_i Z_j e^2/q^2. \tag{3.2.4}$$

In Section II.5, we approximated the electron screening by the ring approximation,

$$\pi_e^*(\vec{q},\nu_n) \simeq \pi_e^o(q,\nu_n) = -2(2\pi)^{-3} \int d\vec{p}\, \frac{n^o(\vec{p}+\vec{q}) - n^o(\vec{p})}{h\nu_n + i\eta - E(\vec{p}+\vec{q}) + E(\vec{p})}, \tag{3.2.5}$$

where η is a small positive parameter. Let μ_e and m_e represent the chemical potential and mass of the electron, respectively, then

$$n^o(\vec{p}) = \exp\{-\beta[E(\vec{p}) - \mu_e]\} - 1, \tag{3.2.6a}$$

$$E(\vec{p}) = h^2p^2/2m_e. \qquad (3.2.6b)$$

At this point we digress and examine the divergence difficulties that one finds in a simple perturbation expansion of the free energy of a system of classical point charges immersed in a uniform neutralizing background. The divergences are due to the long-range nature of the Coulomb interaction. Also there are short-distance divergences, again due to the Coulomb interaction which has an infinity at $\vec{x}=0$. The divergences were removed by nodal expansions developed independently by Abe[41], Meeron[42], and Friedman.[43] In these developments the divergences are systematically removed in two steps: (1) chains of Coulomb interactions are summed to give screened interactions, and (2) the resulting ladder diagrams with screened interactions are summed. Step (1) introduces the Debye screening length, and step (2) gives βe^2 as the distance of closest approach.

We return to Eq.(2.5.7) and the retardation effects in U_τ^Σ. We point out that the contributions from the retardation effects, $U_\tau^\Sigma(\nu\neq 0)$, play no role in cutting off[57] the long range divergences. Also note that the electron proper polarization part introduced in Eq.(3.2.1) and evaluated in the ring approximation is given by,[54]

$$\pi_e^o(q,\nu_n) = (z_e/\Lambda_e^3)\int_o^{\beta h} d\tau\, \exp\left\{ \frac{h^2q^2\tau(\beta-\tau)}{2m_e\beta h} + \frac{2\pi i n\tau}{\beta h} \right\}$$

$$= (z_e\beta/\Lambda_e^3)\left\{1 + \frac{\beta h^2q^2}{4\pi^2m_en^2} - \frac{3\beta^2h^4q^4}{2\pi^4m_e^2n^4} + \ldots\right\};\ \text{for } n\neq 0 \qquad (3.2.7)$$

Since the primary contribution in the integral in Eq.(2.5.7b) is for $q<q_\Sigma$, where $1/q_\Sigma$ is the range of the interaction defined in Eq.(2.5.7d), we neglect all but the first term in Eq.(3.2.7) for $1/q_\Sigma >> \Lambda_e$.

The accuracy of this assumption has not been determined for $1/q_\Sigma \gtrsim \Lambda_e$, however, the approximation $U_\tau^\Sigma(\nu=0)$ appears to contain[60] all the essential effects of correlations due to both the long range part of the Coulomb interaction and exchange.

With this simplification, the classical limit for the ions is easily taken using the rules in Section II.6. We find that the resulting expression for the microfield distribution $Q_i^\Sigma(\vec{\varepsilon})$ is similar to that in Eq.(1.1.1),

$$Q_i^\Sigma(\vec{\varepsilon}) = Z_N^{-1} \int\cdots\int d\vec{r}_o\cdots d\vec{r}_N \exp\{-\beta V^{\Sigma o}\}\delta(\vec{\varepsilon}-\vec{E}_i^\Sigma). \tag{3.2.8}$$

However, the results in Eq.(3.2.8) involve the effective interaction

$$V^{\Sigma o} = \sum_{0=i<j} u^{\Sigma o}(|\vec{r}_i-\vec{r}_j|) \tag{3.2.9a}$$

$$u_{ij}^{\Sigma o}(q) = v_{ij}(q)\{1 - v_{ee}(q)\pi_e^o(q,\nu=0)\}^{-1} \tag{3.2.9b}$$

where $u_{ij}^{\Sigma o}(q)$ is the Fourier transform of $u^{\Sigma o}(\vec{r}_i-\vec{r}_j)$.

The shielded interaction in Eq.(3.2.9) may be rewritten in the form

$$u_{ij}^{\Sigma o}(q) = 4\pi Z_i Z_j e^2\{1 + \lambda^2(q)q^2\}^{-1} \tag{3.2.10}$$

where $\lambda(q)$ can be interpreted as a q-dependent screening length defined by

$$\lambda(q) = [-4\pi e^2\pi_e^o(q,0)]^{-1/2}. \tag{3.2.11}$$

The numerical evaluation of $\pi_e^o(q,0)$ is discussed in detail by C. Gouedard and C. Deutsch[61] for an electron gas at any degeneracy. The q-dependence of $\lambda(q)$ is very weak for values of the product $q\lambda(q)$ less than 1. Therefore, it is possible to make the approximation

$$\overset{\Sigma}{u}{}_{ij}^{o}(q) \simeq 4\pi Z_i Z_j e^2 \lambda_o^2 \{1+(\lambda_o q)^2\}^{-1} \tag{3.2.12a}$$

$$\lambda_o = \lambda(q=0) \tag{3.2.12b}$$

For values of the density and temperature considered here, the error introduced by the approximation in Eq.(3.2.12) is less than 1%.

The inverse Fourier transform of Eq.(3.2.12) is easily performed

$$\overset{\Sigma}{u}{}_{ij}^{o}(r) = Z_i Z_j e^2 \exp\{-r/\lambda_o\}/r. \tag{3.2.13}$$

The functional form of Eq.(3.2.13) is similar to Eq.(3.1.5) although there is a difference in the screening length. It can be shown[52,54] that in the high temperature limit λ_o goes to λ_e.

In the next section we calculate the low-frequency microfield for a gas of ions but the ions interact through the effective interaction given in Eq.(3.2.13).

III.3 Numerical Results and Analysis

The formalism developed in Ref. 6 is now easily extended to the case of ions interacting through $\overset{\Sigma}{V}{}^{o}$ as given in Eq.(3.2.9). The results are compared in Figs.(3.1) and (3.2) with a low-frequency microfield calculation which treats the electrons in a Debye-Hückel

theory. The plasma conditions in the figures are for values of the electron plasma parameter, $\Gamma_e = 0.125$ and 0.214, where

$$\Gamma_e = \beta e^2 / r_o \tag{3.3.1}$$

and r_o is the average electron interparticle distance which, for an electron density ρ_e, is defined by

$$4\pi \rho_e r_o^3 / 3 = 1. \tag{3.3.2}$$

The degeneracy parameter, γ, is defined as the ratio of the noninteracting electron gas Fermi temperature to the temperature of the system,

$$\gamma = T_F / T. \tag{3.3.3}$$

From the two figures we see that the quantum corrections to the Debye screening shift the peak of the $P(\varepsilon)$ curves to a higher value of ε. This behavior may be anticipated. In Eq.(3.2.13) λ_o takes into account the fact that the electrons at the bottom of the Fermi momentum distribution are 'frozen' and cannot fully participate in the screening. Therefore, λ_o is larger than λ_e for a given electron temperature and density so that the electron screening is reduced and the ion electric fields are, on the average, larger.

For the cases presented here, the quantum corrections are small. In fact, only for $\gamma \gtrsim 1$ are the effects of the corrections noticeable. It follows that the quantum corrections to the electron screening of the ions are negligible in recent laser-produced plasma experiments,[25] since

in these experiments $\gamma < 0.05$. The results in Figs.(3.1) and (3.2) also indicate that even in future experiments, where denser plasmas are expected, the quantum corrections to the Debye screening will still be small.

Finally, we note that the low-frequency microfields are used in calculating line profiles which in turn are used as a diagnostic tool to measure electron densities and temperature. It is important to investigate how the quantum corrections in the microfield affects the line profiles. We have done this for the Lyman-α and Lyman-β lines of Ar^{+17} and Cl^{+16}. We were limited to electron densities of order 10^{25} electrons/cm^3 because for plasmas more dense than that, the structure of the profile is completely washed out. For the two cases we did calculate, the effect of the quantum corrections in the screening was small, less than 0.1%.

Fig. 3.1 $P(\varepsilon)$ curves for $\Gamma_e = 0.125$. ε is in units of ε_o.

For $\gamma = 0.43$; $\rho_e = 10^{25}$ part/cm^3, $\Lambda_e^T/\lambda_o = 0.70$.

For $\gamma = 1.01$; $\rho_e = 1.56 \times 10^{26}$ part/cm^3, $\Lambda_e^T/\lambda_o = 1.03$.

For $\gamma = 1.96$; $\rho_e = 10^{27}$ part/cm^3, $\Lambda_e^T/\lambda_o = 1.22$.

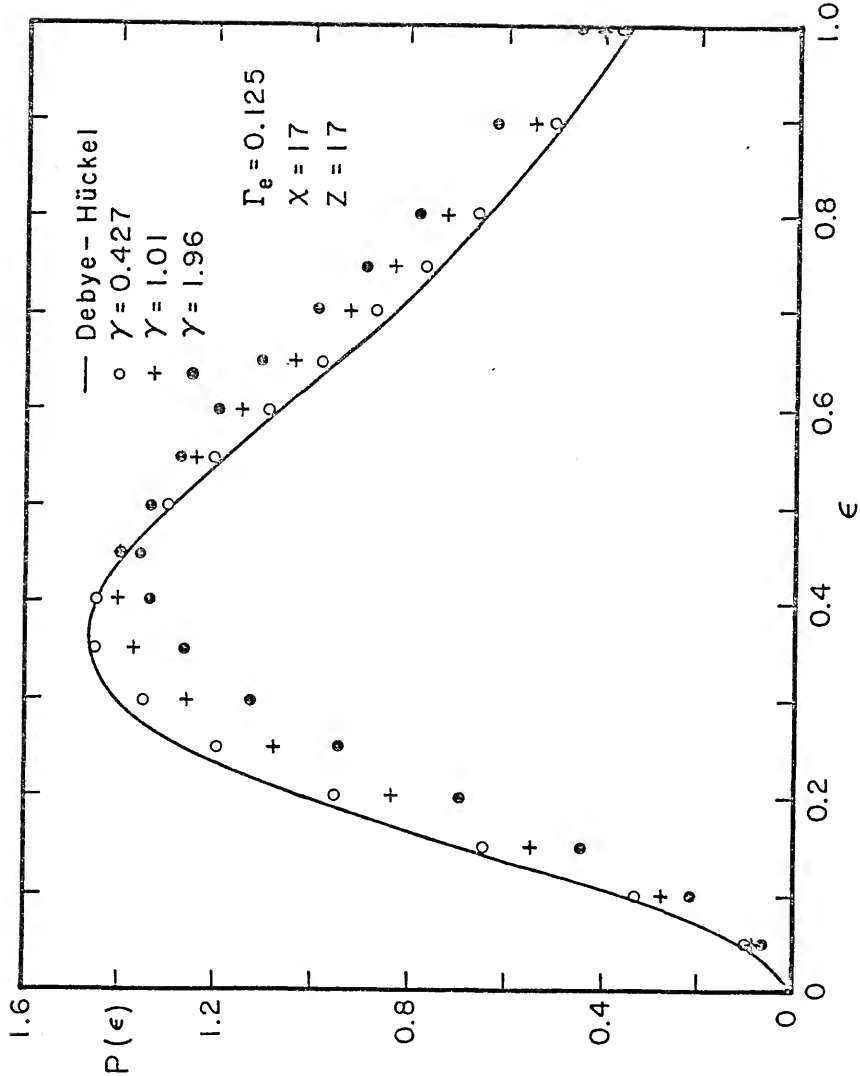
Debye-Hückel
γ = 0.427
γ = 1.01
γ = 1.96
Γe = 0.125
χ = 17
Z = 17
P(ε)
ε
0
0.4
0.8
1.2
1.6
0.2
0.6
1.0

Fig. 3.2 $P(\varepsilon)$ curves for $\Gamma_e = 0.214$. ε is in units of ε_o.

For $\gamma = 0.67$; ρ_e 2 x 10^{24} part/cm^3, $\Lambda_e/\lambda_o = 1.13$.

For $\gamma = 1.23$; $\rho_e = 5 \times 10^{25}$ part/cm^3, $\Lambda_e/\lambda_o = 1.41$.

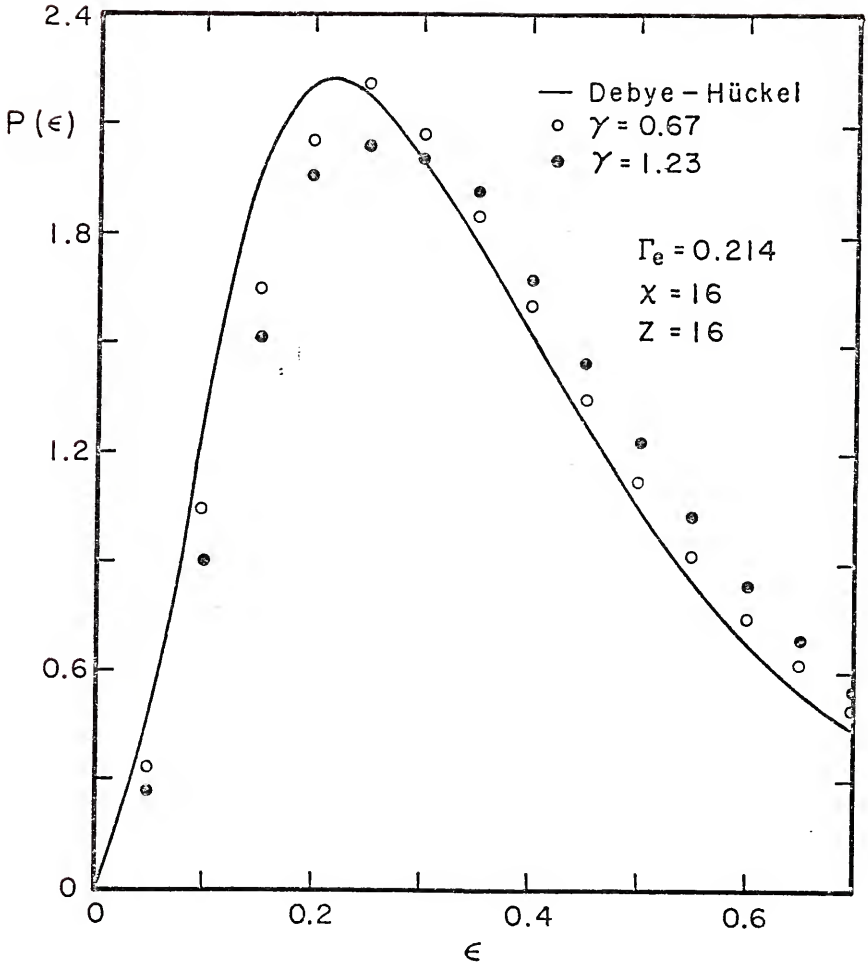
2.4
1.8
1.2
0.6
0
P(ϵ)
0
0.2
0.4
0.6
ϵ
Debye – Hückel
γ = 0.67
γ = 1.23
Γe = 0.214
χ = 16
Z = 16

CHAPTER IV
INTEGRAL EQUATION METHOD

In this chapter we propose an integral equation approach to evaluate the microfield distribution function define in Eq.(1.1.4). This involves expressing $T(\ell)$ in terms of a two-body function. This two-body function is formally identical to the radial distribution function (RDF), therefore, it is amenable to integral equation techniques.

The resulting expression for $T(\ell)$ involves an integration over a so-called coupling parameter. This integration may be performed in the hypernetted-chain[62-65] (HNC) approximation to the two-body function, simplifying the expression for $T(\ell)$. For simplicity we treat the same system as in Chapter I.

IV.1 Connection with the Chemical Potential

It was first noted by Morita[8] that the virial expansion for $T(\ell)$ is formally similar to that of the excess chemical potential, $\delta\mu$, which is defined by

$$\exp(\beta\delta\mu) = Z_N/\Omega Z_{N-1}. \tag{4.1.1}$$

A comparison of Eqs.(1.1.6) and (4.1.1) shows that the two quantities are indeed similar.

It is possible to write $\delta\mu$ in terms of the RDF.[59] Introduce the coupling parameter ζ, which varies from 0 to 1 and which has the effect of replacing the interaction of some particle, say 1, with the jth particle of the system by $\zeta v(r_{ij})$. In terms of this coupling parameter, then, the potential energy for the system is written in the form

$$V = \sum_{j=2}^{N} \zeta v(r_{ij}) + \sum_{2\leq i<j\leq N} v(r_{ij}). \tag{4.1.2}$$

Clearly,

$$Z_N(\zeta=1) = Z_N \tag{4.1.3a}$$

and

$$Z_N(\zeta=0) = \Omega\, Z_{N-1}. \tag{4.1.3b}$$

Eq.(4.1.3) can be used in Eq.(4.1.1) with the result[59]

$$\delta\mu = \rho \int_0^1 d\zeta \int d\vec{r}\; v(r)g(r;\zeta) \tag{4.1.4}$$

where $g(r;\zeta)$ is the RDF for particle 1 an any other particle.

The RDF can be evaluated with integral equation techniques. In the framework of the HNC approximation, it has been shown[65] that the integration over the parameter ζ can be done.

We have intentionally omitted details in this section since the steps are discussed elsewhere.[59,65] In addition, almost the identical steps will be shown in the next sections for the $T(\ell)$ case.

IV.2 The Two-Body Function $g(\vec{r};\zeta)$

Because of the similarity between $T(\ell)$ and $\delta\mu$, it is possible to write an expression like Eq.(4.1.4) for $T(\ell)$. To do this we introduce the parameter ζ which is defined as the magnitude of the vector $\vec{\ell}$,

$$\zeta = |\vec{\ell}|. \tag{4.2.1}$$

We may rewrite the 'potential' $V(\ell)$ defined in Eq.(1.1.8) as

$$V(\zeta) = V + ie^{-1}\zeta\hat{\ell}\cdot\vec{E}, \tag{4.2.2a}$$

where

$$\vec{E} = \sum_{j=1}^{N} \vec{\varepsilon}(\vec{r}_{jo}) \tag{4.2.2b}$$

and $\hat{\ell}$ is the unit vector in the direction of $\vec{\ell}$. The definition of $Z_N(\zeta)$ follows from Eq.(4.2.2),

$$Z_N(\zeta) = \int d\vec{r}_0 d\vec{r}_1 \cdots d\vec{r}_N \exp\{-\beta V(\zeta)\}. \tag{4.2.3}$$

If we let ζ vary from 0 to ℓ in Eqs.(4.2.2) and (4.2.3), then we can take the field in and out of the expressions by varying ζ. This is useful since now we may write for $T(\ell)$,

$$\ell n T(\ell) = \ell n[Z_N(\zeta=\ell)/Z_N(\zeta=0)]$$

$$= \int_0^{\ell} d\zeta \, \frac{\partial \ell n \, Z_N(\zeta)}{\partial \zeta}$$

$$= \int_o^{\ell} d\zeta \int d\vec{r}_o \cdots d\vec{r}_N \left\{ \sum_{j=1}^{N} i\hat{\ell}\cdot\vec{\varepsilon}(\vec{r}_{jo})/e \right\} e^{-\beta V(\zeta)}/Z_N(\zeta)$$

$$= \rho \int_o^{\ell} d\zeta \int d\vec{r}\, \psi(\vec{r}) g(\vec{r};\zeta) \qquad (4.2.4)$$

where

$$\psi(\vec{r}) = i\hat{\ell}\cdot\vec{\varepsilon}(\vec{r})/e \qquad (4.2.5)$$

and

$$g(\vec{r};\zeta) = \Omega^2 \int d\vec{r}_2 \cdots d\vec{r}_N \; e^{-\beta V(\zeta)}/Z_N(\zeta). \qquad (4.2.6)$$

The function $g(\vec{r};\zeta)$ reduces to the usual RDF for $\zeta=0$. Hence, for arbritary values of ζ, $g(\vec{r};\zeta)$ is simply the 'RDF' for the zeroth particle and any other particle where the system interacts through the 'potential' $V(\zeta)$.

In Eq.(4.2.4) the effect of the neutralizing background has not been included. The background term is given by

$$\int d\vec{r}\, \psi(\vec{r}) = \psi(\vec{q}=0) \qquad (4.2.7)$$

where $\psi(\vec{q})$ is defined as the Fourier transform

$$\psi(\vec{q}) = \int d\vec{r}\; e^{-i\vec{q}\cdot\vec{r}}\; i\hat{\ell}\cdot\vec{\varepsilon}(\vec{r})$$

$$= \hat{\ell}\cdot\vec{q}v(q)/e \qquad (4.2.8)$$

and

$$v(q) = 4\pi e^2/q^2. \tag{4.2.9}$$

With the background term included in Eq.(4.2.4), we may write

$$\ell n T(\ell) = \rho \int_0^{\ell} d\zeta \int d\vec{r}\, \psi(\vec{r}) h(\vec{r};\zeta) \tag{4.2.10}$$

where $h(\vec{r};\zeta)$ is the total correlation function and is defined by

$$h(\vec{r};\zeta) = g(\vec{r};\zeta) - 1 \tag{4.2.11}$$

Eq.(4.2.10) is the main result of this chapter; we have expressed $T(\ell)$ in terms of a two-body function. This form has the advantage that knowledge of a two-body function gives $T(\ell)$ exactly, in contrast to Refs. 3 and 5 which require knowledge of many-body functions. Of course, the price to be paid for this advantage is the integration over the parameter ζ which requires $g(\vec{r};\zeta)$ for all values of ζ between 0 and ℓ.

IV.3 The Holtsmark Limit

It is instructive to examine Eq.(4.2.10) in the Holtsmark or high temperature limit where the total correlation function is given by,

$$\lim_{T\to\infty} h(\vec{r};\zeta) = e^{\zeta\psi(\vec{r})} - 1; \tag{4.3.1}$$

this expression can be substituted into Eq.(4.2.10) and we find

$$\lim_{T\to\infty} \ell n T(\ell) = \rho \int_0^{\ell} d\zeta \int d\vec{r}\psi(\vec{r})[e^{\zeta\psi(\vec{r})} - 1]$$

$$= \rho \int_0^{\ell} d\zeta \int d\vec{r} \frac{\partial}{\partial\zeta}[e^{\zeta\psi(\vec{r})} - 1]$$

$$= \rho \int d\vec{r}\,[e^{\ell\psi(\vec{r})} - 1]. \qquad (4.3.2)$$

The expression for $T(\ell)$ is then given as

$$T(\ell) = \exp\{\rho \int d\vec{r}[e^{i\vec{\ell}\cdot\vec{\varepsilon}(\vec{r})} - 1]\} \qquad (4.3.3)$$

which is the correct Holtsmark limit.[5,31]

IV.4 HNC Approximation

The total correlation function is amenable[59] to integral equation techniques. In this section we evaluate the correlation function in the HNC approximation. As mentioned earlier, in this approximation the integration over the parameter ζ can be performed.

A second reason for treating Eq.(4.2.10) in the HNC approximation is the fact that this approximation has been sucessful in obtaining the RDF and the internal energy for the one component plasma for values of $a>2.0$. It is possible that with the use of the HNC approximation we may be able to calculate microfield distributions for these values of a.

First, we write $h(\vec{r};\zeta)$ in the form

$$h(\vec{r};\zeta) = \exp\{-\beta v(r) + \zeta\psi(\vec{r}) + \gamma(\vec{r};\zeta)\} \qquad (4.4.1)$$

which formally defines $\gamma(\vec{r};\zeta)$. The function $\gamma(\vec{r};\zeta)$ is given by the sum

of nodal and bridge graphs,[62-65]

$$\gamma(\vec{r};\zeta) = N(\vec{r};\zeta) + B(\vec{r};\zeta) \tag{4.4.2}$$

In Eq. (4.4.2) $N(\vec{r};\zeta)$ is the sum of the nodal graphs; nodal graphs are those irreducible graphs[11] for which all possible paths from one rooted point[11] to the other have at least one vertex in common. The term $B(\vec{r};\zeta)$ is the sum of the bridge graphs; bridge graphs are irreducible graphs and there are at least two alternate paths between the rooted vertices. Examples of nodal and bridge graphs are presented in Figs.(4.1a) and (4.1b), respectively.

In the HNC approximation[62-65], $B(\vec{r};\zeta)$ is set equal to zero. Then,

$$\gamma(\vec{r};\zeta)\big|_{HNC} = N(\vec{r};\zeta) = h(\vec{r};\zeta) - c(\vec{r};\zeta) \tag{4.4.3}$$

where $c(\vec{r};\zeta)$ is the direct correlation function and is defined by the Ornstein-Zernike[66] equation ,

$$h(\vec{r}_{10};\zeta) = c(\vec{r}_{10};\zeta) + \rho \int d\vec{r}_2 \; c(r_{12})h(\vec{r}_{20};\zeta) \tag{4.4.4a}$$

$$h(r) = c(r) + \rho \int d\vec{r}' \; c(|\vec{r}-\vec{r}'|)h(r). \tag{4.4.4b}$$

In Eq.(4.4.4b) h(r) and c(r) are the total and direct correlation functions for ζ equal to zero.

Introducing the Fourier tranforms and using the convolution theorem we get for Eq.(4.4.4)

Fig. 4.1 (a) Some examples of Nodal graphs.

(b) Some examples of Bridge graphs.

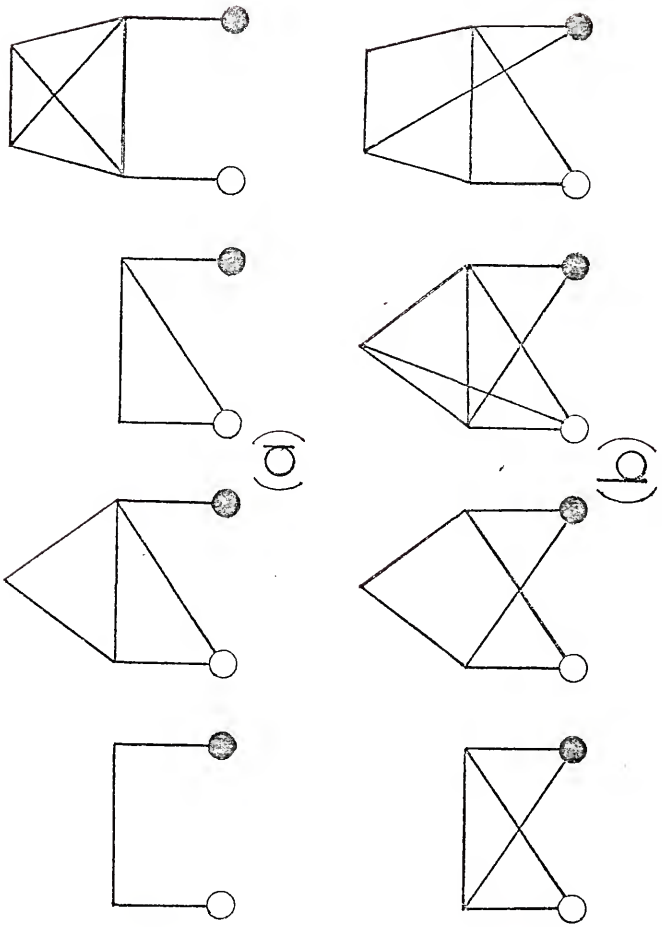
(a)
(b)

$$h(\vec{k};\zeta) = c(\vec{k};\zeta) + \rho c(k)h(\vec{k};\zeta) \tag{4.4.5a}$$

$$h(k) = c(k) + \rho c(k)h(k). \tag{4.4.5b}$$

Using Eqs.(4.4.3) and (4.4.5) we may write

$$N(\vec{k};\zeta) = \rho h(\vec{k};\zeta)[h(k) - N(k)], \tag{4.4.6}$$

where

$$N(k) = N(\vec{k};\zeta=0) = h(k) - c(k). \tag{4.4.7}$$

It is now possible[65] to simplify Eq.(4.2.10) by noting that we may write from Eq.(4.4.1),

$$\frac{\partial h(\vec{r};\zeta)}{\partial \zeta} = \{u(\vec{r}) + \frac{\partial \gamma(\vec{r};\zeta)}{\partial \zeta}\}\{h(\vec{r};\zeta) + 1\}, \tag{4.4.8}$$

$$\psi(\vec{r})h(\vec{r};\zeta) = \frac{\partial h(\vec{r};\zeta)}{\partial \zeta} - \psi(\vec{r}) - \frac{\partial \gamma(\vec{r};\zeta)}{\partial \zeta} - h(\vec{r};\zeta)\frac{\partial \gamma(\vec{r};\zeta)}{\partial \zeta}. \tag{4.4.9}$$

Substitution of Eq.(4.4.9) into Eq.(4.2.10) leads to

$$\ell nT(\ell) = \rho \int d\vec{r}\{[h(\vec{r};\ell) - h(r)] - [\gamma(\vec{r};\ell) - \gamma(r)]$$

$$- \rho \int_0^{\ell} d\zeta \int d\vec{r}\, h(\vec{r};\zeta)\frac{\partial \gamma(\vec{r};\zeta)}{\partial \zeta}. \tag{4.4.10}$$

In arriving at Eq.(4.4.10) we have used the identity,

$$\int d\vec{r}\ \psi(\vec{r}) \sim \int_0^{r_\Omega} dr \int_{-1}^{1} d\eta\ \eta = 0, \tag{4.4.11}$$

where r_Ω is the radius of the volume of the system, Ω.

If we calculate $\ell nT(\ell)$ in the HNC approximation, then

$$\ell nT(\ell)\big|_{NHC} = \rho \int d\vec{r}\{[h(\vec{r};\ell) - N(\vec{r};\ell)] - [h(r) - N(r)]\}$$

$$-\rho \int_0^{\ell} d\zeta \int d\vec{r}\ h(\vec{r};\zeta)\ \frac{\partial N(\vec{r};\zeta)}{\partial \zeta}\ . \tag{4.4.12}$$

We can simplify[65] the term involving the integration over ζ,

$$\rho \int_0^{\ell} d\zeta \int d\vec{r}\ h(\vec{r};\zeta)\ \frac{\partial N(\vec{r};\zeta)}{\partial \zeta}$$

$$= (2\pi)^{-3}\rho \int_0^{\ell} d\zeta \int d\vec{k}\ h(-\vec{k};\zeta)\ \frac{\partial h(\vec{k};\zeta)}{\partial \zeta}\ [h(k)-N(k)]$$

$$= [2(2\pi)^3]^{-1}\rho \int_0^{\ell} d\zeta \int d\vec{k}\ \frac{\partial}{\partial \zeta}\ h(-\vec{k};\zeta)h(\vec{k};\zeta)[h(k) - N(k)]$$

$$= (\rho/2) \int d\vec{r}\ \{h(\vec{r};\ell)N(\vec{r};\ell) - h(r)N(r)\}. \tag{4.4.13}$$

Substituting Eq.(4.4.13) into Eq.(4.4.12) gives

$$\ell nT(\ell)\big|_{HNC} = \rho\{[c(\vec{k}=0;\ell) - c(k=0)]$$

$$-\frac{1}{2} \int d\vec{r}\ [h(\vec{r};\ell)N(\vec{r};\ell) - h(r)N(r)] \tag{4.4.14}$$

The result in Eq.(4.4.14) can be used in Eq.(1.1.4) to evaluate the microfield distribution function. The quantities c, h, and N in

Eq.(4.4.14) are to be evaluated in the HNC framework. These quantities with $\ell=0$ can be calculated to high accuracy by the method of Ng.[67] The ℓ-dependent quantities are directionally dependent which may lead to complications. Another source of difficulties are the quantities $c(\vec{k}=0;\ell)$ and $c(k=0)$. Although their difference is finite, each one separately is divergent. This singular behavior is due to the long (non-integrable) range of the Coulomb interaction.

IV.5 Alternate Approximation Schemes

Up to now we have emphasized the treatment of Eq.(4.2.10) by integral equations, in particular the HNC approximation. It is also possible that starting from Eq.(4.2.10) and some approximation to the correlation function other than HNC, we may obtain alternate methods for calculating microfield distribution functions for $a > 2.0$. We now discuss several such approximations.

The first and simplest approximation to $g(\vec{r};\zeta)$ is given by the Debye-Hückel theory. We obtain

$$g(\vec{r};\zeta) \simeq \exp\{-\beta[1 + i\zeta\hat{\ell}\cdot\vec{\nabla}]W(r)\}, \tag{4.5.1}$$

where $W(r)$ is the potential of mean force[59] which in this approximation is given by

$$-\beta W(r) \simeq -\Lambda\exp\{-\beta r/\lambda\}/r. \tag{4.5.2}$$

The plasma parameter is defined by

$$\Lambda = \beta e^2/\lambda = a^3/3 \tag{4.5.3}$$

where λ is the Debye screening length. Because of the simple form of $g(\vec{r};\zeta)$ in Eq.(4.5.1), the ζ-integration is easily performed in Eq. (4.2.10). The numerical results for the microfield distribution in this approximation are in good agreement with the results of Hooper[5] only for values of $a < 0.4$. This is not surprising since the Debye-Hückel theory is only valid for weakly coupled plasmas, $\Lambda << 1$.

In order to improve the Debye-Hückel results, several theories[7-20] have been proposed to compute higher order terms in the parameter Λ. The application of such theories to $g(\vec{r};\zeta)$ is complicated by the angular dependence of the field terms in $V(\zeta)$. As a simplification, we assume that $g(\vec{r};\zeta)$ has the functional form given in Eq. (4.5.1) and we evaluate $W(r)$ to second order in Λ. We found that the numerical results for $P(\varepsilon)$ in this approximation do not sufficiently improve on the Debye-Hückel results.

Finally, we considered an analytic fit[68-70] to the Monte Carlo RDF data in order to obtain $W(r)$. For the one value of $a=5.0$, the results for $P(\varepsilon)$ were not in good agreement with Monte Carlo calculations[15] of the microfield distribution.

We believe that the reason that the latter approximation to $g(\vec{r};\zeta)$ fails to give good numerical results is due to the approximate functional form in Eq. (4.5.1). This functional form implicitly assumes that the field term in $V(\zeta)$ gives a weakly coupled 'interaction' and neglects ladders in this field terms. Consequently the strong fields are underestimated. In fact, all three approximations above give $P(\varepsilon)$ curves which have a maximum at too small a value of ε. At present we

are investigating how to incorporate strong field effects into $g(\vec{r};\zeta)$ without introducing cumbersome and lengthy numerical calculations.

APPENDIX A
DERIVATION OF EFFECTIVE INTERACTIONS

In this appendix we are concerned with explicit evaluation of the effective interactions, $\beta u^s(\vec{r},\ell)$, indicated in Fig.(1.3). The simple chain summation which produces $-\beta u^s(\vec{r},\ell)$ has the following analytic form

$$- \beta u^s(\vec{r}_{01},\ell) = - \beta u(\vec{r}_{01},\ell) - \beta \sum_{j=2}^{\infty} (-\beta\rho)^{j-1} \int \cdots \int d\vec{r}_2 \cdots d\vec{r}_j \times$$

$$\times u(\vec{r}_{02},\ell) v(r_{23}) \cdots v(r_{j1})$$

$$= \{1 - \frac{i\vec{\ell}\cdot\vec{\nabla}_0}{e\beta}\}\{ - \beta u(r_{01}) - \beta \sum_{j=2}^{\infty} (-\beta\rho)^{j-1} \int \cdots \int d\vec{r}_2 \cdots d\vec{r}_j \times$$

$$\times u(r_{02}) v(r_{23}) \cdots v(r_{j1}). \qquad \text{(A-1)}$$

Introduce the Fourier transforms

$$p(\vec{r}) = \frac{1}{(2\pi)^3} \int d\vec{q}\ e^{i\vec{q}\cdot\vec{r}}\ p(\vec{q}), \qquad \text{(A-2)}$$

where $p(\vec{r})$ stands for u, u^s, v, or v^s. Then, using the Faultung (convolution) method obtain for the transform of $u^s(\vec{r}_{10},\ell)$

$$u^s(\vec{q},\ell) = \{1 - \frac{\vec{\ell}\cdot\vec{q}}{e\beta}\}\ u(q)/\varepsilon(q). \qquad \text{(A-3)}$$

The dielectric response function ε and the transform of u(r) and v(r)

are defined by

$$\varepsilon(q) = 1 + \rho\beta\, v(q),$$

$$u(q) = \frac{4\pi e^2 \alpha^2}{q^2[\alpha^2 + (\lambda q)^2]},$$

$$v(q) = \frac{4\pi e^2}{q^2}. \qquad \text{(A-4)}$$

Similarly, for the noncentral effective interaction,

$$v^s(q) = v(q)/\varepsilon(q). \qquad \text{(A-5)}$$

Eqs.(A3) and (A5) may be inverse transformed to yield

$$u^s(r) = \frac{\alpha^2}{\alpha^2 - 1}\left(\frac{e^2}{r}\right)\left\{e^{-r/\lambda} - e^{-\alpha r/\lambda}\right\},$$

$$v^s(r) = \frac{e^2 e^{-r/\lambda}}{r}. \qquad \text{(A-6)}$$

APPENDIX B
EVALUATION OF $T_o(\ell)/T_o(0)$

In this appendix we evaluate the term $T_o(\ell)/T_o(o)$. To do this we first evaluate the ring graph sum presented in Fig.(1.4a),

$$\ell n\, T_o(\ell) = \frac{-\rho\beta^2}{2} \sum_{j=1}^{\infty} (-\beta\rho)^{j-1} \frac{(j-1)!}{j!} \int \cdots \int d\vec{r}_1 \cdots d\vec{r}_j$$

$$\times\, u(\vec{r}_{01},\ell)v(r_{12}) \cdots v(r_{j-1,j})u(\vec{r}_{j0},\ell) \qquad \text{(B-1)}$$

As in Appendix A, we make use of the Fourier transforms to write

$$\ell n\, T_o(\ell) = \frac{-\rho\beta^2}{2} \int \frac{d\vec{q}}{(2\pi)^3}\, u(\vec{q},\ell)u(-\vec{q},\ell)\varepsilon^{-1}(q). \qquad \text{(B-2)}$$

Since $T_o(o)$ simply requires $T_o(\ell=0)$ it follows that

$$\ell n\, T_o(\ell)/T_o(0) = \frac{-\rho\beta^2}{2} \int \frac{d\vec{q}}{(2\pi)^3}\, \varepsilon^{-1}(q)\, \{u(\vec{q},\ell)u(-\vec{q},\ell) - u^2(q)\}$$

$$= \frac{-\rho\beta^2}{2} \int \frac{d\vec{q}}{(2\pi)^3}\, \varepsilon^{-1}(q)\, \left(\frac{\vec{\ell}\cdot\vec{q}}{e\beta}\right)^2 u^2(q)$$

$$= \frac{-\alpha^3 a L^2}{4(\alpha^2+1)^2} = -\gamma L^2, \qquad \text{(B-3)}$$

where in Eq.(B3)

$$L = \ell\varepsilon_o;\ a = r_o/\lambda;\ \varepsilon_o = e/r_o^2, \qquad \text{(B-4)}$$

and r_o is the ion sphere radius defined by the expression

$$\frac{4\pi}{3} r_o^3 \rho = 1. \qquad \text{(B-5)}$$

APPENDIX C
CALCULATION OF γ_1

In this appendix we evaluate the integrals in Eq.(1.2.17),

$$-\gamma_1 L^2 = \frac{\rho^2\beta^2}{2}\int d\vec{r}_{10}d\vec{r}_{20}\ [\beta v^s(r_{12})]^2/2$$

$$\times\ \{u^s(\vec{r}_{10};\ell)u^s(\vec{r}_{20};\ell) - u^s(r_{10})u^s(r_{20})\}. \qquad (C\text{-}1)$$

Introduce the Fourier transforms defined in Eq.(A-2), and get

$$\rho F[\beta^2 v^s(r)^2/2] = \frac{a^3}{6\lambda q}\tan^{-1}(\lambda q/2), \qquad (C\text{-}2a)$$

$$F[\beta u^s(\vec{r};\ell)] = \frac{-4\pi\alpha^2 a^3\lambda^3}{3[1+(\lambda q)^2][\alpha^2+(\lambda q)^2]}\left\{1+\frac{3\lambda}{a}\vec{L}\cdot\vec{q}\right\} \qquad (C\text{-}2b)$$

where F denotes the Fourier transform. Substituting Eq.(C-2) into Eq.(C-1) we find

$$-\gamma_1 L^2 = \frac{\alpha^4 a^9\lambda^6\rho}{54\pi}\int d\vec{q}\ \frac{\tan^{-1}(\lambda q/2)}{\lambda q[1+(\lambda q)^2][\alpha^2+(\lambda q)^2]^2}$$

$$\times\ \left\{(1+\frac{3}{a}\vec{L}\cdot\lambda\vec{q})(1-\frac{3}{a}\vec{L}\cdot\lambda\vec{q})-1\right\}$$

$$= \frac{-\alpha^4 a^2}{8\pi^2}\int d\vec{Q}\ \frac{\tan^{-1}(Q/2)}{Q(1+Q^2)(\alpha^2+Q^2)^2}\ (\vec{L}\cdot\vec{Q})^2$$

$$= \frac{a^2\alpha^4 L^2}{12(\alpha^2-1)^3}\left\{(\alpha^2+1)\ell n(\frac{3}{2+\alpha})+\frac{(\alpha^2+1)(2\alpha+1)}{3(\alpha+2)}\right\} \qquad (C\text{-}3)$$

which defines γ_1 as given in Eq.(1.2.17).

APPENDIX D

CALCULATION OF THE FUNCTIONS t(x) AND p(x)

In this appendix we evaluate the function t(x) and p(x). These functions appear as a result of performing the $\vec{r}_1$ integrations in Eq.(1.2.16). The funciton t(x) is defined as

$$(1 - \frac{i\vec{\ell}}{\beta e} \cdot \vec{\nabla}_o)t(x_{20}) = \frac{-\rho\beta^3}{2} \int d\vec{r}_1 \; u^s(\vec{r}_{10},\ell)[v^s(r_{12})]^2$$

$$= (1 - \frac{i\vec{\ell}}{\beta e} \cdot \vec{\nabla}_o)(\frac{-\rho\beta^3}{2}) \int d\vec{r}_1 \; u^s(r_{10})[v^s(r_{12})]^2. \qquad \text{(D-1)}$$

From Eq.(D-1) we get for $t(x_{20})$

$$t(x_{20}) = \frac{-\rho\beta^3}{2} \int d\vec{r}_1 \; u^s(r_{10})[v^s(r_{12})]^2$$

$$= \frac{-a^6}{72\pi} (\frac{\alpha^2}{\alpha^2-1}) \int d\vec{x}_{10} \left\{ \frac{e^{-ax_{10}} - e^{-a\alpha x_{12}}}{x_{10}} \right\} \frac{e^{-2ax_{12}}}{x_{12}^2} . \qquad \text{(D-2)}$$

Or,

$$t(x) = \frac{a^5}{36x} (\frac{\alpha^2}{\alpha^2-1}) \{ e^{ax} E_1(3ax) + e^{-ax}[\ell n 3 - E_1(ax)]$$

$$- \frac{e^{a\alpha x}}{\alpha} E_1\big((2+\alpha)ax\big) + e^{-a\alpha x}[\ell n(\frac{2+\alpha}{2-\alpha}) - E_1\big((2-\alpha)ax\big)] \}, \qquad \text{(D-3)}$$

where in Eq.(D-2)

$$E_1(y) \equiv \int_y^\infty dt\ e^{-t}/t\ ;\ y > 0. \tag{D-4}$$

In getting Eq.(D-3) we used bipolar coordinates.[71] The result in Eq. (D-3) is valid for $\alpha<2$ only.

The function p(x) is defined as follows

$$\left(1 - \frac{i\hat{\ell}}{\beta e} \cdot \vec{\nabla}_o\right) t(x_{20}) = t(x_{20}) + iLp(x_{20}) \frac{\vec{L}\cdot\vec{x}_{20}}{|\vec{L}|\ |\vec{x}_{20}|} \tag{D-5}$$

With the help of the identity

$$\frac{\partial E_1(by)}{\partial y} = \frac{-e^{-by}}{y}\ , \tag{D-6}$$

we get from Eq.(D-5)

$$p(x) = x^{-1}\left\{\frac{-a^4}{12}\left(\frac{\alpha^2}{\alpha^2-1}\right)\left[e^{ax}E_1(3ax) - e^{-ax}\left(\ell n3 - E_1(ax)\right)\right.\right.$$

$$\left. - e^{a\alpha x}E_1\left((2+\alpha)ax\right) - e^{-a\alpha x}\left(\ell n\left(\frac{2+\alpha}{2-\alpha}\right) - E_1\left((2-\alpha ax\right)\right)\right]$$

$$\left. - \frac{3t(x)}{a^2}\right\}. \tag{D-7}$$

APPENDIX E
PROJECTION OPERATOR TECHNIQUES

A complete knowledge of the state of a system is not always necessary for the calculation of observable quantities pertaining to the system. A simple example is the case where the operator D is diagonal in some representation, in that representation, we need only the diagonal part of the density operator to calculate,

$$\langle D \rangle = \mathrm{Tr}\rho D. \tag{E-1}$$

Zwanzig[45-48] has developed a formal procedure for obtaining an integro-differential equation which governs the time development of the 'relevant' part of any operator satisfying the equation (in units such that h=1)

$$\frac{\partial}{\partial t} D(t) = i[H,D(t)]. \tag{E-2}$$

In the Liouville representation this equation takes the form

$$\frac{\partial}{\partial t} D(t) = LD(t), \tag{E-3}$$

where L is the Liouville operator defined by

$$LD(t) = i[H,D(t)]. \tag{E-4}$$

Let the relevant part of the quantity D(t) be pulled out by a projection operator P, and called it $D_1(t)$. The remainder of D(t) is the irrelevant part $D_2(t)$,

$$D(t) = D_1(t) + D_2(t), \tag{E-5a}$$

$$D_1(t) = PD(t), \tag{E-5b}$$

and

$$D_2(t) = (1-P)D(t). \tag{E-5c}$$

Assume that P is not a function of time. Then, we may operate on Eq. (E-3) and find

$$\frac{\partial}{\partial t} D_1(t) = PL[D_1(t) + D_2(t)], \tag{E-6}$$

and

$$\frac{\partial}{\partial t} D_2(t) = (1-P)L[D_1(t) + D_2(t)]. \tag{E-7}$$

The solutions to Eq.(E-7) are formally given by

$$D_2(t) = \exp\{(1-P)Lt\}D_2(t=0)$$

$$+ \int_o^t ds \exp\{1-P)LS\}(1-P)L\, D_1(t-s). \tag{E-8}$$

Substitution of Eq.(E-8) into Eq.(E-6) gives an integro-differential equation for $D_1(t)$,

$$\frac{\partial}{\partial t} D_1(t) = PLD_1(t) + PL \int_o^t ds \exp\{(1-P)LS\}(1-P)D_1(t-s), \quad \text{(E-9)}$$

where we have assumed that $D_2(t=0)=0$. This condition is satisfied by all cases considered in this dissertation.

Now we define the Laplace transform

$$D_1(\omega) = \int_o^\infty dt\ e^{i\omega t} D_1(t). \quad \text{(E-10)}$$

Taking the Laplace transform of Eq.(E-9) and using the convolution theorem we get

$$-iD_1(t=0) + \omega D_1(\omega) = iPLD_1(\omega)$$

$$+ iPL\int_o^\infty dt\ \exp\{(i\omega + (1-P)L)t\}(1-P)LD_1(\omega)$$

$$= iP\{L - \frac{L}{\omega} \sum_{n=0}^{\infty} \left[\frac{i(1-P)L}{\omega}\right]^n (1-P)L\}D_1(\omega). \quad \text{(E-11)}$$

Using the relation

$$\frac{1}{\omega} \sum_{n=0}^{\infty} \left[\frac{i(1-P)L}{\omega}\right]^n = \left[\omega - i(1-P)L\right]^{-1}, \quad \text{(E-12)}$$

we get after some algebra,

$$-iD_1(\omega) = \left[\omega - PT(\omega)\right[^{-1} D_1(t=0), \quad \text{(E-13)}$$

where

$$T(\omega) = iP\left[L + L\left\{\omega - i(1-P)L\right\}^{-1}(1-P)iL\right]. \qquad \text{(E-14)}$$

The results in Eqs.(E-13) and (E-14) are used repeatedly in Chapter II.

REFERENCES

1. J. Holtsmark, Ann. Phys. 58, 577 (1919).

2. A.A. Broyles, Phys. Rev. 100, 1181 (1955).

3. B. Mozer and M. Baranger, Phys. Rev. 115, 521 (1959).

4. B. Mozer and M. Baranger, Phys. Rev. 118, 626 (1960).

5. C.F. Hooper, Jr., Phys. Rev. 149, 177 (1966).

6. C.F. Hooper, Jr., Phys. Rev. 165, 215 (1968).

7. R.J. Tighe and C.F. Hooper, Jr., Phys. Rev. A15, 1773 (1977).

8. T. Morita, Prog. Theor. Phys. 23, 1211 (1960).

9. J.E. Mayer, J. Chem. Phys. 18, 1426 (1950).

10. J.E. Mayer and M.G. Mayer, Statistical Mechanics (John Wiley and Sons, New York, 1940).

11. E.E. Salpeter, Ann. Phys. 5, 183 (1958).

12. H. Cramer, Mathematical Methods of Statistics (Princeton University Press, Princeton, 1957), p. 211.

13. W.J. Swiatecki, Proc. Roy. Soc. (London) A205, 238 (1951).

14. The Bateman Manuscript Project, Higher Transcendental Functions (California Institute of Technology, Pasadena, California, 1953), Vol. II, Chap. VII.

15. H.E. DeWitt, (private communication).

16. J.C. Weisheit and E.L. Pollock, Spectral Line Shapes Ed. B. Wende, Walter de Guyter and Co., Berlin, 1981).

17. D.L. Bowrs and E.E. Salpeter, Phys. Rev. 119, 1180 (1960).

18. H.E. DeWitt, Phys. Rev. 140A, 466 (1965).

19. E.G.D. Cohen and T.J. Murphy, Phys. Fluids 12, 1404 (1969).

20. F. del Rio and H.E. DeWitt, Phys. Fluids 12, 1404 (1969).

21. H.R. Griem, Plasma Spectroscopy (McGraw-Hill, New York, 1964).

22. H. Baranger, Atomic and Molecular Processes (Ed. D.R. Bates, Academic Press, New York, 1962), Chap. 13.

23. J. Cooper, Plasma Spectroscopy, Rep. Progr. Phys. 29, 35 (1966).

24. A. Hauer, Bull. Am. Phys. Soc. 24, 1053 (1979).

25. B. Yaakobi, R.L. McCrory, S. Skupsky, J.A. Delettrez, P. Burke, H. Deckman, C.F. Hooper, and J.M. Soures, Phys. Rev. Lett. 44, 1072 (1980).

26. U. Fano, Lectures on the Many-Body Results (Ed. E.R. Caianiello, Academic Press, New York, 1964), Vol. 2.

27. L. Klein, J. Quant. Spectros. Rad. Trans. 9, 199 (1969).

28. A. Royer, Phys. Rev. A6, 1741 (1972).

29. T.W. Hussey, J.W. Dufty and C.F. Hooper, Jr., Phys. Rev. A12, 1084 (1977).

30. E. Smith, C.R. Vidal, and J. Cooper, J. Res. Natn. Bur. Stand. 73A, 389 405 (1969).

31. H.R. Griem, Spectral Line Broadening (Academic Press, New York, 1974).

32. R.J. Tighe, dissertation (University of Florida, 1977).

33. E.W. Smith, J. Cooper, W.R. Chapell, and T. Dillon, J. Quant. Spectros. Rad. Trans. 11, 1547 (1971).

34. J.E. Whalen, dissertation (University of Florida, 1972).

35. T.W. Hussey, J.W. Dufty, and C.F. Hooper, Jr., Phys. Rev. A16, 1248 (1977).

36. J.W. Dufty and D.B. Boercker, J. Quant. Spectros. Rad. Trans. 16, 1065 (1978).

37. P. Debye and E. Hückel, Physik Z. 24, 185 (1923).

38. J.W. Dufty, Phys. Rev. 187, 305 (1969).

39. R.J. Tighe and C.F. Hooper, Jr., Phys. Rev. A17, 410 (1978).

40. L.A. Woltz, R.F. Joyce, and C.F. Hooper, Jr., Spectral Line Shapes (Ed. B. Wende, Walter de Gruyter and Co., Berlin, 1981).

41. R. Abe, Progr. Theor. Phys. 22, 213 (1959).

42. E. Meeron, Phys. Fluids 1, 139 (1958).

43. H.F. Friedman, Mol. Phys. 2, 23 (1959).

44. T.J. Buckholtz, Ann. Phys. 86, 197 (1973).

45. R. Zwanzig, Lectures in Theoretical Physics (Eds. W.E. Downs and J. Downs, Interscience Publishers, Inc., New York, 1961), Vol. 3.

46. R. Zwanzig, J. Chem. Phys. 33, 1338 (1960).

47. R. Zwanzig, Phys. Rev. 124, 938 (1961).

48. R. Zwanzig, Physica 30, 1109 (1964).

49. R.M. Wilcox, J. Math. Phys. 8, 962 (1967).

50. N.N. Bogliubov, Lectures on Quantum Statistics (Gordon and Preach, New York, 1967), Vol. 1.

51. A.A. Abrikosov, L.P. Gorkov, and I.E. Dzyaloshinski, Methods of Quantum Field Theory in Statistical Physics (Dover Publications, Inc., New York, 1975).

52. A.L. Fetter and J.D. Walecka, Quantum Theory of Many-Particles Systems, (McGraw-Hill, New York, 1971).

53. R.D. Mattuck, A Guide to Feynman Diagrams in the Many-Body Problem (McGraw-Hill, New York, 1967).

54. A. Isihara, Statistical Physics (Academic Press, New York, 1971).

55. D. Bohm and D. Pines, Phys. Rev. 92, 609 (1953).

56. A. Isihara, Phys. Rev. 178, 412 (1969).

57. H.E. DeWitt, J. Math. Phys. 7, 616 (1966).

58. R.A. Smith, Ann. Phys. 81, 402 (1973).

59. D.A. McQuarrie, Statistical Mechanics (Harper and Ross, New York, 1971).

60. D.B. Boercker, dissertation (University of Florida, 1977).

61. C. Gouedard and C. Deutsch, J. Math. Phys. 19, 32 (1978).

62. J.M.J. van Leeneven, J. Groeneveld, and J. de Boer, Physica 25, 792 (1959).

63. T. Morita and K. Hiroike, Prog. Theor. Phys. 23, 1003 (1960).

64. E. Meeron, J. Math. Phys. 1, 192 (1960).

65. M. Bauss and J.P. Hansen, Rep. Progr. Phys. 59, 1 (1980).

66. L.S. Orstein and F. Zernike, Proc. Acad. Sci. (Amsterdam) 17, 793 (1914).

67. K.C. Ng, J. Chem. Phys. 61, 2680 (1974).

68. B. Jancovici, J. Statist. Phys. 17, 357 (1977).

69. H.E. DeWitt, Proc. Orleans Nato Summer Institute of Strongly Coupled Plasmas (Ed. Kalman, Plenum Press, 1978).

70. V. Canuto, Astrophys. J. 159, 641 (1970).

71. T.L. Hill, Statistical Mechanics (McGraw-Hill, New York, 1956).

BIOGRAPHICAL SKETCH

Carlos A. Iglesias was born on November 25, 1951 in La Habana, Cuba. In March of 1962 he was exiled to the United States. After receiving his secondary education at Miami Senior High School in June of 1969 he began his college education at Miami-Dade Junior College. Later he transferred to the University of Florida, Gainesville, where he received his Bachelor of Science degree in physics in June, 1973. From September of that year until the present, he has been a graduate student in the Department of Physics at the University of Florida.

I certify that I have read this study and that in my opinion it conforms to acceptable standards of scholarly presentation and is fully adequate, in scope and quality, as a dissertation for the degree of Doctor of Philosophy.

Charles F. Hooper, Jr., Chairman
Professor of Physics

I certify that I have read this study and that in my opinion it conforms to acceptable standards of scholarly presentation and is fully adequate, in scope and quality, as a dissertation for the degree of Doctor of Philosophy.

James W. Dufty
Professor of Physics

I certify that I have read this study and that in my opinion it conforms to acceptable standards of scholarly presentation and is fully adequate, in scope and quality, as a dissertation for the degree of Doctor of Philosophy.

Pradeep Kumar
Assistant Professor of Physics

I certify that I have read this study and that in my opinion it conforms to acceptable standards of scholarly presentation and is fully adequate, in scope and quality, as a dissertation for the degree of Doctor of Philosophy.

James R. Brookeman
Associate Professor of Physics

I certify that I have read this study and that in my opinion it conforms to acceptable standards of scholarly presentation and is fully adequate, in scope and quality, as a dissertation for the degree of Doctor of Philosophy.

Charles A. Burnap
Assistant Professor of Mathematics

This dissertation was submitted to the Graduate Faculty of the Department of Physics in the College of Liberal Arts and Sciences and to the Graduate Council, and was accepted as partial fulfillment of the requirements for the degree of Doctor of Philosophy.

_____

Dean for Graduate Studies
and Research

UNIVERSITY OF FLORIDA
3 1262 08553 1852